EFDA–JET–R(12)01

S. Bellocchi

Neutron-γ Pulse Shape Discrimination with NE213 Liquid Scintillator: Comparison of Different Sampling Rate/Bit Resolution Digital Acquisition Systems Datasets

Neutron-γ Pulse Shape Discrimination with NE213 Liquid Scintillator: Comparison of Different Sampling Rate/Bit Resolution Digital Acquisition Systems Datasets

S. Bellocchi

[1]*EURATOM/UKAEA Fusion Association, Culham Science Centre, OX14 3DB, UK.*

Neutron-γ Pulse Shape Discrimination with NE213 liquid scintillator: comparison of different sampling rate/bit resolution digital acquisition systems datasets.

Dr Sara Bellocchi

Energetic Engineering “Laurea Magistrale”

Granted a scholarship at the

Nuclear Fusion EFDA-JET Laboratory, Culham, Oxfordshire (UK)

Research title according to n°3 argument

“Measurements of Plasma diagnostic”

Dr Andrea Murari Resident tutor at the Jet Laboratory

Dr Luca Giacomelli Resident tutor at the Jet Laboratory

Dr Michela Gelfusa Resident tutor at Tor Vergata University of Rome

Prof Pasquale Gaudio Resident tutor at Tor Vergata University of Rome

Introduction

In nuclear fusion experiments, neutrons are created in the reactions between fuel hydrogen isotops; deuterium-tritium and deuterium-deuterium fusion reactions give respectively rise to neutrons of 14 and 2.5 MeV kinetic energy. Neutron spectrometry represents thus a tool for obtaining important information on the fuel ion composition, velocity distribution and temperature of fusion plasmas.

Moreover in a fusion reaction gamma-rays generated both in the plasma source and by interaction of the neutrons with the materials in the shielding and the environment, contaminate neutron fields. Since neutron spectrometry is possible only if neutron- and photon-induced events can be well identified then detectors with n-γ discrimination capability are needed.

Mechanisms for detecting neutrons in matter are based on indirect methods. The neutron can be scattered by a nucleus, transferring some of its kinetic energy. If the neutron energy reaches the keV range, enough energy is transferred in the elastic scattering and the recoiling nucleus ionizes the material surrounding the point of interaction. This mechanism is only efficient for neutrons interacting with light nuclei. In fact, only hydrogen and helium nuclei are light enough for practical detectors.

Hydrogen-containing scintillators allow the detection of high energy neutrons using proton recoil and successful applications have been reported with organic scintillators for neutron energies > 1 MeV [1-4].

The use of these detectors poses some problem. Their material composition affects γ sensitivity. Plastic scintillators feature low γ sensitivity different from liquid scintillating materials (i.e., NE213). The pulse shape of the signal induced by the radiation interactions in the detector depends also on the nature of the radiation itself (neutrons or γ's for this study). With increasing stopping power the fraction of excitations with longer lifetimes (delay fluorescence) increases.
For NE213 liquid scintillators, gamma-ray induced fast electrons generate a larger fraction of their scintillation light in the prompt component as compared with neutron induced recoil proton events; Pulse Shape Discrimination (PSD) methods allow for the identification of the incoming radiation.

NE213 liquid scintillator has been extensively used in mixed radiation fields of neutrons and γ-rays [5-8].

Compact NE213 liquid scintillators are implemented in the 19 channel neutron camera (KN3) at the Joint European Torus (JET). They have been operational since 1996, collecting data during the experimental campaigns performed since then.

The present work reports on the analysis neutron and γ pulse shapes produced in KN3 channel 4 using the ^{241}Am/^{9}Be neutron source (i.e., reference source for the calibration of the KN3 diagnostic) and recorded with two different digital acquisition systems.

The first digital acquisition system is the oscilloscope TekTronix TDS3034B (OSC) [9] with operated at 5Gsamples/s sampling rate and 8 bit resolution. The second digital acquisition system (DAQ) designed by ENEA Frascati [10] was recently implemented on KN3 with the aim of replacing the old analog acquisition system. The DAQ featurs in 200Msamples/s sampling rate and 14 bit resolution.

The oscilloscope data has been analyzed using different time resolutions (from 0.2 ns to 5 ns) to compare with the KN3 DAQ of 5 ns time resolution aiming at the comparison of the two acquisitions system, in order to investigate the impact of time resolution/amplitude (bit) resolution on the n-γ discrimination capability.

In this work, the PSD is conducted by using the charge comparison method. Digitized signals are integrated within two different time intervals (gates) as implemented in the analysis of the DAQ data. Two different gates, *Short Gate (S)* and the *Long Gate (L)*, along the pulse shape, are considered.

The ratio S/L can be exploit as an efficient tool to classify neutron rather than γ-ray, being $L_n >> L_\gamma$, $S/L|_n << S/L|_\gamma$. Various S-L gate combinations have been in the OSC and DAQ data analysis. Depending on the choice of S and L, neutron and γ-ray events can give rise to two well separated lobes in the S/L distribution. The neutron and γ lobes are analyzed in terms of Gaussian distributions which parameters are used to quantify the efficiency of n-γ discrimination of the PSD method. This is summarized by the Figure of Merit (FoM) [12], which has been calculated exploiting three different methods of analysis of the events S/L distributions obtained for various S-L gate combinations:

1. Gaussian fit of the neutron lobe and real γ lobe;
2. Gaussian fits of the neutron and γ lobes separately;
3. Double Gaussian fit of the full S/L distribution.

The FoM was also tested using the γ/n branching ratio of ^{241}Am/^{9}Be neutron source.

The analysis was carried out considering different time resolutions for the OSC data (from 0.2 ns to 5 ns) down sampling the recorded waveforms. For each OSC time resolution, since different position of the starting sample result in a different pulse shape of the same waveform, the effects of the sampling sequence was also investigated.

The PSD analysis was performed using scripts in *Python* and using its tools [11].

This work consisted in the comparison of the performance of the OSC and DAQ systems with respect to n-γ discrimination. In particularly the following aspects have been investigated:

- The optimal S-L gate settings for both OSC and DAQ for channel 4 of the KN3 system;
- Whether the high sampling rate of the oscilloscope is beneficial in γ discrimination though a lower amplitude (bit) resolution with respect to the KN3 DAQ system.

The analysis and main results are presented in the following.

Statistical method application

In the previous chapters liquid scintillating detectors were introduced and the application in neutron detection and spectroscopy in γ-ray mixed fields described. NE231 liquid scintillator is a common choice for n-γ pulse shape discrimination and they are implemented in the 19 channel neutron camera (KN3) on JET. This thesis reports on the analysis of the neutron and γ pulse shapes recorded with two different digital acquisition systems.

The first digital acquisition system considered is the oscilloscope TekTronix TDS3034B (OSC) [9] of 5Gsamples/s sampling rate and 8 bit resolution. The second digital acquisition system (DAQ) [10] was recently implemented on KN3 with the aim of replacing the old analog acquisition system. The DAQ features consists in 200Msamples/s sampling rate and 14 bit resolution. The sampling frequency affects the waveform details recorded in the data, as shown in Figure 5.1.

For clearness, we will name with OSC the data recorded with the oscilloscope and with DAQ waveforms recorded with the KN3 acquisition system.

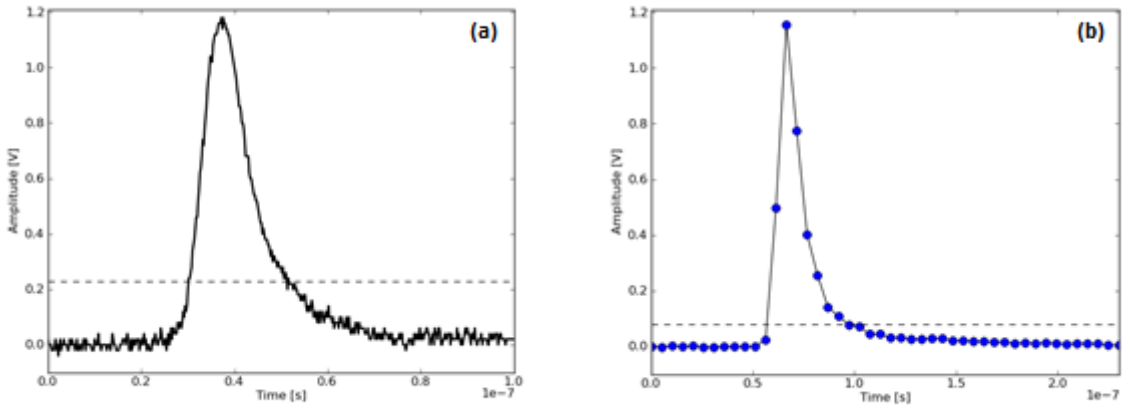

Figure 5.1. Examples of OSC (a) and DAQ (b) data in V versus time.

As we mentioned in the previous chapters the NE213 n-γ discrimination capability can be exploited using different analysis methods which make use of the differences in pulse shape due to the light emission induced in the scintillator by the type of radiation.

In this work, the PSD is conducted by using the charge comparison method as implemented by the KN3 DAQ system. The method consists in the integration of the digitized signals within two different time intervals (gates). Two different gates, *Short Gate (S)* and the *Long Gate (L)*, along the

pulse shape are considered. The pulse area (i.e., sum of the pulse amplitude values) within τ_S and τ_L is calculated and referred to as S and L. For each pulse shape the pair (S,L) is selected (according to procedure described on pages 14 - 17), the pulse height in S and L gates are considered and their ratio is (from now on indicted as S/L). The distribution of S/L for the data set will feature peaks depending on the nature of the detected particle. Both S and L gates in the KN3 DAQ system processing method are set from the peak position of the waveform.

Figure 5.2 shows normalized neutron and γ average pulses, with respectively their slow and fast trailing edge due to the different combination of light decay components in the scintillator. S and L labeled in the figure represent the short and the long integration gate previously mentioned.

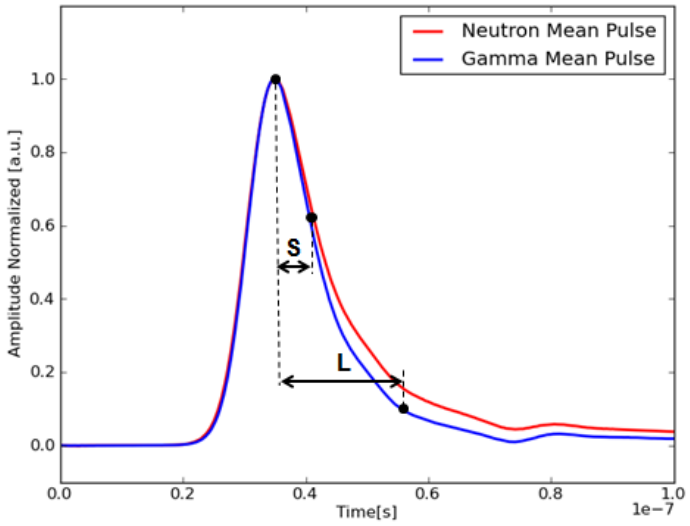

Figure 5.2. Short and long gates for normalized neutron and γ pulses.

The ratio S/L can be exploit as an efficient tool to classify neutron rather than γ-ray: being $L_n >> L_\gamma$, $S/L|_n << S/L|_\gamma$. Extending this procedure to the whole database, by using the same S-L gate combination, one can determine the S/L distribution (see Figure 5.3). Depending on the choice of S and L, neutron and γ-ray events can give rise to two lobes if the S-L gates are chosen correctly. The lobes are shaped as a Gaussian distribution which parameters are used to quantify the efficiency of n-γ discrimination of the PSD method. This is summarized by the Figure of Merit (FoM) defined as (see Chapter 3) [12]:

$$FoM = \frac{S_{n-\gamma}}{FWHM_\gamma + FWHM_n}$$

where $S_{n-\gamma}$, $FWHM_n$ and $FWHM_\gamma$ are the separation between the centroids and the full-width at half-maximum of the neutron and γ-rays lobes, respectively.

Varying the S and L distribution assumes different shapes. Here an example S/L distribution for S = 8.8 ns and L = 51.4 ns, obtained considering the OSC data recorded at 5 GSamples/s for 0.2ns.

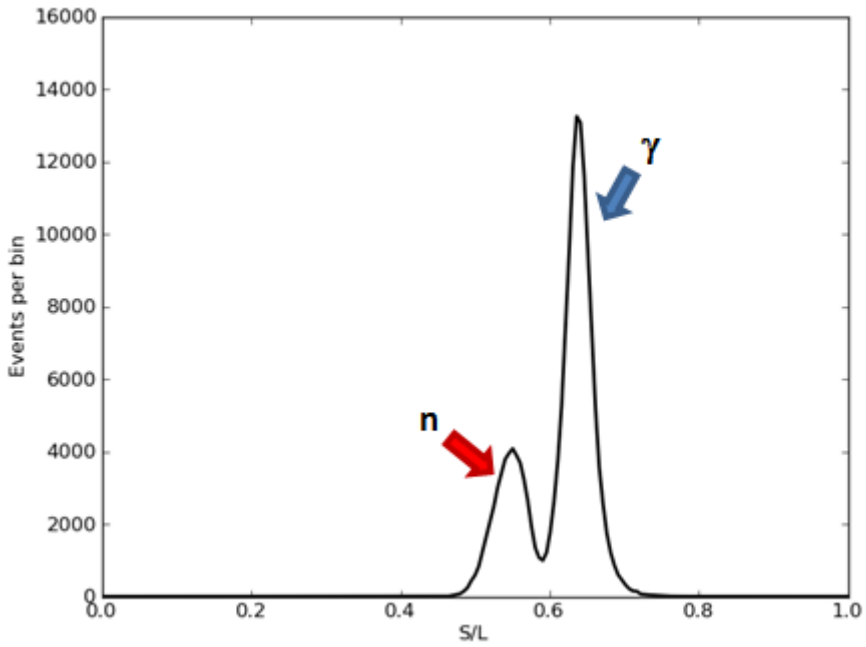

Figure 5.3. S/L distribution obtained with gate method for PSD; the lobe of the left-hand side corresponds to neutrons events while the one to the right-hand side to γ-ray events.

The aim of this thesis consists in the comparison of the performance of the OSC and DAQ systems with respect to n-γ discrimination. Two main aspects will been investigated:

- Whether an higher sampling rate of the oscilloscope is beneficial in γ suppression though a lower bit resolution with respect to the KN3 DAQ system;
- The optimal S-L gate settings for both OSC and KN3 DAQ system.

Americium-Beryllium neutron source

Data analyzed in this thesis refer to an ^{241}Am/^{9}Be neutron source. Americium acts as the alpha emitter:

$$^{241}_{95}Am \rightarrow ^{237}_{93}Np + ^{4}_{2}He + \gamma$$

Neutrons are produced through the ${}^{9}_{4}Be$ (α,n)${}^{12}_{6}C$ reaction:

$$ {}^{4}_{2}He + {}^{9}_{4}Be \rightarrow {}^{12}_{6}C + {}^{1}_{0}n + \gamma $$

^{241}Am decays to a chain of daughter products and contribute with gamma-ray background to that produced in ${}^{9}_{4}Be(\alpha, n)$ reactions.

These γ-source can be roughly estimated by the branching ratios of γ-ray decays produced in ^{241}Am/^{237}Np alpha decay. Figure 5.4 provides ^{237}Np metastable states; next to each energy level the energy of gamma-ray (keV), alpha particle energy (MeV) and the branching ratio are respectively reported.

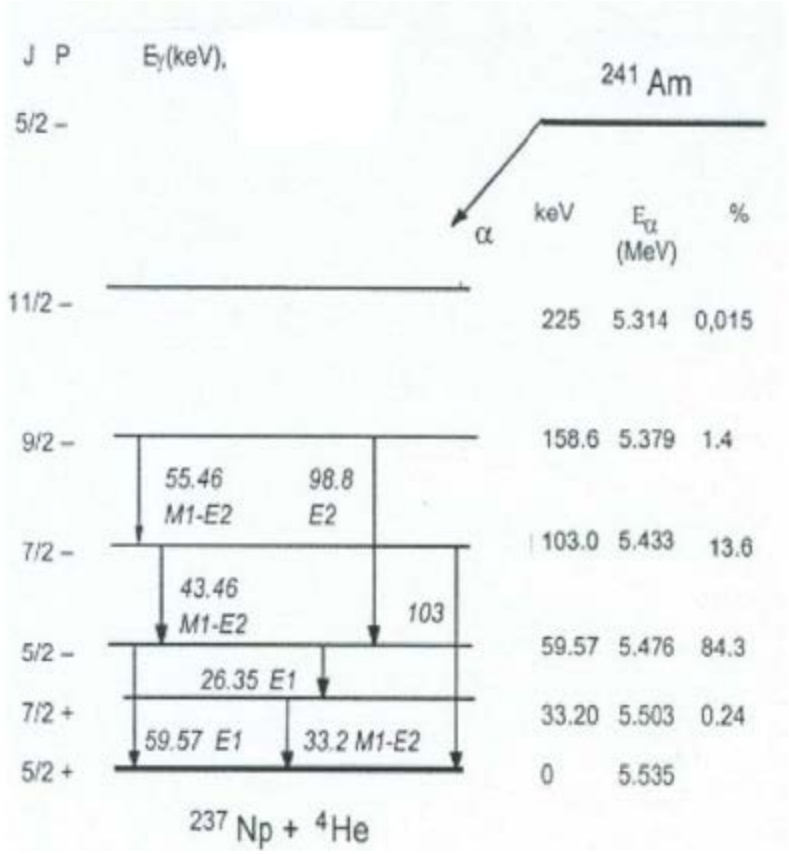

Figure 5.4. Metastable states in ^{241}Am/^{237}Np alpha decay nuclear process. The energy of gamma-ray and alpha and branching ratios are specified beside the energy levels represent respectively.

If the nucleus is in a metastable level it can decay to intermediate levels through γ emission. In this way the number of gamma-ray produced in ^{241}Am/^{237}Np decay can be seen as a probability distribution. From 1 to 4 γ's can be produced in the ^{241}Am/^{237}Np reaction per neutron, with their respective probabilities. The maximum probability lies around 1-2 gamma rays. The total number of gamma-ray produced can be obtained considering also one γ emitted in the ${}^{9}_{4}Be(\alpha, n){}^{12}_{6}C$ reaction. This lead to a γ-ray background estimated as 2-3 γ per neutron.

Figure 5.5 shows the neutron source deployment device, that allows two $^{241}Am/^{9}Be$ sources to move through the vertical and horizontal camera. The source was positioned on KN3 channel 4 and the analysis refers to this data collected with both OSC and DAQ.

Figure 5.5. $^{241}Am/^{9}Be$ neutron source deployment device. The arrow indicates the position of the source in the horizontal camera, where the channel 4 is located.

Since we know gamma-rays and neutrons produced by the $^{241}Am/^{9}Be$ neutron source in their ratio, we consider the idea of "testing" the FoM validity by its comparison with the γ-rays and neutron events ratio that will be derived from each FoM. Hereafter we will name *R* the gamma-neutron ratio. If this latter falls in the range expected from the branching ratio, i.e. R = 2-3, the FoM can be effectively considered a representative tool for n-γ pulse shape discrimination, otherwise the next larger value compatible with the gamma-neutron ratio expected will be considered.

Pulse analysis and PSD have been brought about by using the programming language *Python* and its tools [11].

Next sections describe the algorithm developed for the analysis and the results obtained for OSC and DAQ data respectively. A comparison between the two data acquisition systems is discussed in the last section.

Algorithm description

The signals induced in the KN3 scintillators by the n and γ emission of the $^{241}Am/^{9}Be$ source have been used for this analysis. The output signal for KN3 channel 4 were fed into OSC and DAQ systems separately.

The dataset consists of 202000 OSC waveforms and 217192 DAQ waveforms.

For the hardware acquisition the threshold was set at 80 mV for the DAQ dataset and at 230 mV for the OSC one.

A Python script [11] has been developed for the analysis of the database. Each waveform of the dataset (OSC or DAQ) is read out and baseline reduced considering the average offset of 100 (OSC) and 12 (DAQ) samples in the pre-trigger region. Once the peak is determined, from its position the area within the short and long gates is calculated. The area is obtained by summation of amplitudes values of the waveform of the samples included in the S and L gates, respectively. The S/L ratio is determined for each waveform of the dataset, which results in the S/L distribution. The distribution reflects the goodness of PSD according to the S and L gate adopted. In order to remove small glitches and have a robust analysis of the S/L distribution shape, smoothing is applied. To calculate FoM the parameters $S_{n-\gamma}$, $FWHM_n$ and $FWHM_\gamma$ are needed to be evaluated.

If two maxima exist in the smoothed histogram, the algorithm determines the minimum between the maxima as the lowest value in the real curve. This value is considered in first approximation as the end of the neutron lobe and the beginning of the gamma one. The maximum and its position for the two lobe are named respectively $x_{n_{peak}}$ and $x_{\gamma_{peak}}$, $y_{n_{peak}}$ and $y_{\gamma_{peak}}$.

Three different methods of analysis of the S/L distribution have been considered to determine these values and calculate FoM:

4. Gaussian fit of the neutron lobe and considering the real gamma lobe (named as Fit N).
5. Gaussian fit of both neutron and gamma lobes individually (named as Fit NG).
6. Double Gaussian fit of both the neutron and gamma lobes together (named as Fit All).

In Fit N the Gaussian fit of the neutron lobe provides $y_{n_{peak}}$, $x_{n_{peak}}$ and σ_n. The Gaussian fit function is:

$$n_{gauss_{fit}} = p_{guess}[0] \cdot e^{-\frac{(x-p_{guess}[1])^2}{2 \cdot p_{guess}[2]^2}}$$

where $p_{guess}[0:2]$ are the initial guess values, corresponding respectively $y_{n_{peak}}$, $x_{n_{peak}}$ and σ_n taken from the real curve. The standard deviation initial guess value σ_n is determined through:

$$(x_{n_{peak}} - x_{0.5n_{peak}}) \cdot \frac{2}{2.335}$$

where $x_{0.5n_{peak}}$ is the position of the first point on the neutron lobe higher than the half the maximum with $x_{0.5n_{peak}} < x_{n_{peak}}$.

The script makes use of a Gaussian fit routine which minimizes the χ^2. When the fit converges to the optimal solution, the Gaussian function is determined and, from σ_n , it results:

$$FWHM_n = 2 \cdot \sqrt{2 \cdot \ln(\sigma)} = 2.355\sigma_n$$

Concerning the γ lobe of the distribution, it was found that its shape is particularly peaked for most of the S-L gate combinations. This could hamper the convergence of the Gaussian fit. For this reason, the $FWHM_\gamma$ is determined from the real curve as:

$$(x_{\gamma_{peak}} - x_{0.5\gamma_{peak}}) \cdot 2$$

where $x_{0.5\gamma_{peak}}$ is the position of the first point on the gamma lobe higher than the half the maximum with $x_{min} < x_{0.5\gamma_{peak}} < x_{\gamma_{peak}}$. The difference between centroids is then evaluated as:

$$S_{n-\gamma} = x_{\gamma_{peak}} - x_{n_{peak}}$$

Figure 5.6 gives an example S/L distribution, where the neutron fit and the parameters needed for the FoM are pointed out.

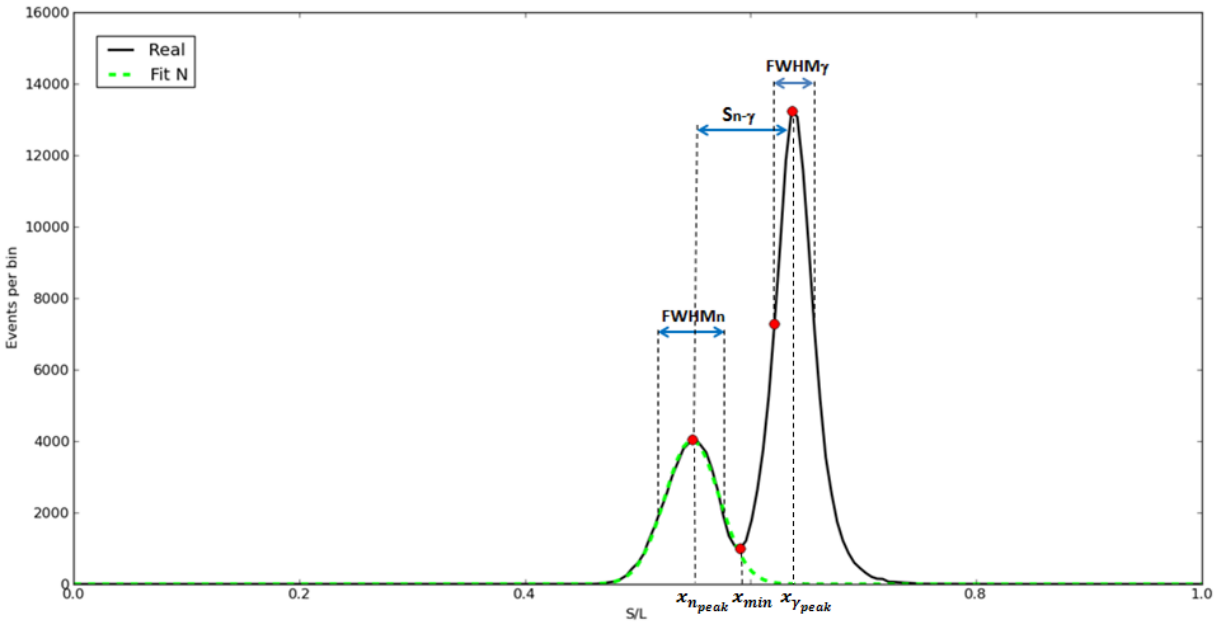

Figure 5.6. Example of Fit N method.

Fit N exploits a Gaussian fit of the neutron and gamma lobe separately:

$$n_{gauss_{fit}} = p_{n_{guess}}[0] \cdot e^{-\frac{(x - p_{guess}[1])^2}{2 \cdot p_{guess}[2]^2}}$$

$$\gamma_{gauss_{fit}} = p_{\gamma_{guess}}[0] \cdot e^{-\frac{(x-p_{guess}[1])^2}{2 \cdot p_{guess}[2]^2}}$$

An initial guess vector is now determined also for the gamma lobe. In Figure 5.7 the same S/L histogram has been used to highlight the parameters considered.

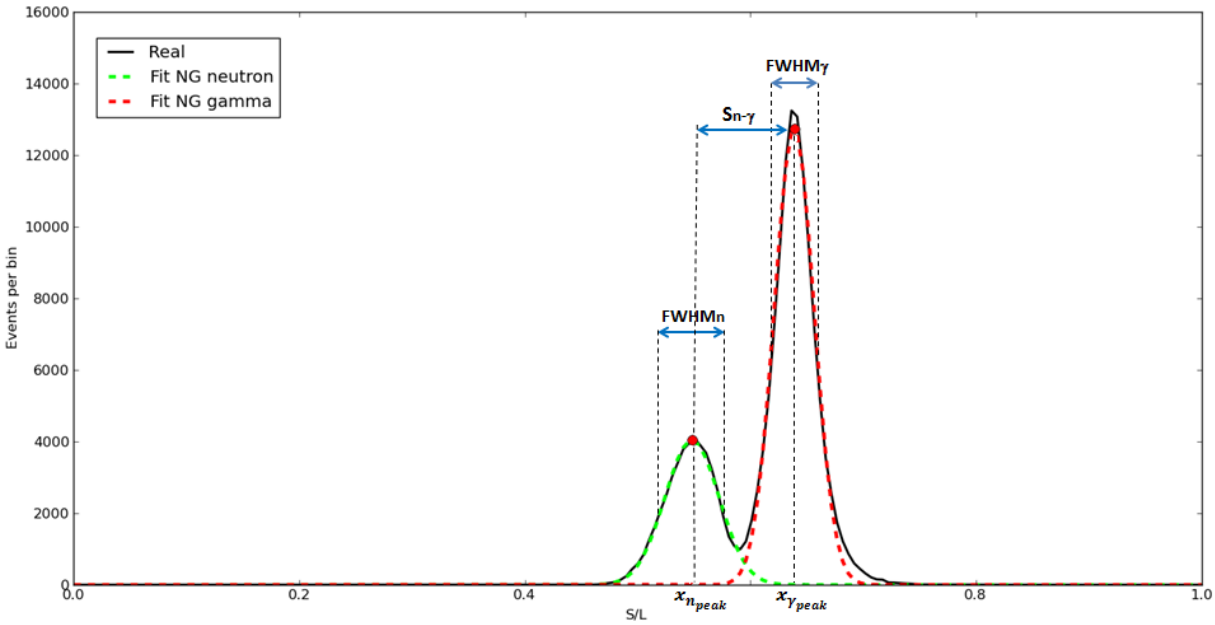

Figure 5.7. Example of Fit NG method.

In Fit All the lobes are fitted simultaneously by a double Gaussian function represented by:

$$y_{gauss\_fit} = n_{gauss\_fit} + \gamma_{gauss\_fit} = p_{n_{guess}}[0] \cdot e^{-\frac{\left(x-p_{n_{guess}}[1]\right)^2}{2 \cdot p_{n_{guess}}[2]^2}} + p_{\gamma_{guess}}[0] \cdot e^{-\frac{\left(x-p_{\gamma_{guess}}[1]\right)^2}{2 \cdot p_{\gamma_{guess}}[2]^2}}$$

where $p_{\gamma_{guess}}$ and $p_{n_{guess}}$ are determined from the real curve in the same way as Fit NG.

Figure 5.8 displays the Fit NG method of analysis using the same S/L distribution.

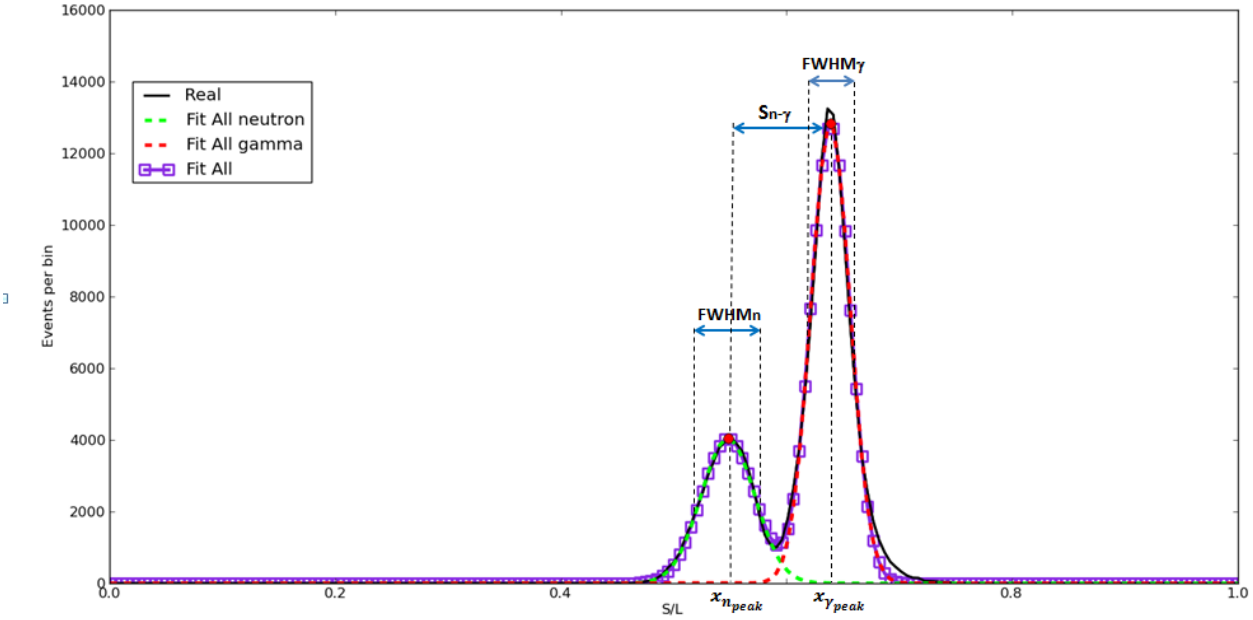

Figure 5.8. Example of Fit All method.

Once the value of the FoM has been determined for a specific S-L combination through the three different methods described, new gates S and L are selected and the analysis repeated.

In this way, the phase space of all S-L gate combination can be explained. The maximum value of FoM corresponds to the optimal S-L gate combination (S_{op}-L_{op}) which maximizes the n-γ discrimination.

Since the ^{241}Am/^{9}Be neutron and γ branching ratio is known, it is possible verify whether the optimal gate combination S_{op}-L_{op} is correct. This is pursued considering the ratio R of the total number of events within the neutron and gamma lobes of the S_{op}/L_{op} distribution, ratio that should match the ^{241}Am/^{9}Be branching ratio.

Few issues to be considered in the analysis are:

1) The number of samples for the gates S and L;

2) The definition of the S/L distribution, i.e., the choice of the binning;

3) The determination of the parameters of interest for FoM.

These topics are discussed in the following sections.

1. S and L gate definition

The gates S and L are chosen to cover the entire range of possible values from the peak to the last sample of the waveform available on the trailing edge. Fixed S to a single value, starting from one sample after the waveform peak, the corresponding L values are in the range from S+1 to the last sample L_{max}. S and L can be expressed in samples (after peak) or in ns depending on the acquisition OSC (0.2 ns) or DAQ (5ns). Considering the *i*-th pulse, the number of samples L_{max} can be determined as:

$$L_{max_i} = Pulselength_i - Peak_i$$

Where $Pulselength_i$ and $Peak_i$ are pulse length and the peak position, respectively.

Anyway, considering the OSC data, which waveforms measure 500 samples, as we mentioned in the previous chapter, due to the amplitude and the offset variation, the maximum can be obtained in different sample positions. This latter condition leads to a variation of L_{max}, depending on the position of the waveform peak, such that L_{max} has to be chosen in the dataset as trade-off between dataset available. L_{max} values account for the entire waveform tail area within L gate. In fact, the higher is L_{max}, the lower is the number of waveforms to be considered in the analysis. On the other hand, the lower L_{max} values, even if they are satisfied by all the waveforms, they do not allow a full evaluation of the tail influence.

We named as *delta* the difference between the pulse length and the peak position; the distributions of delta for the different OSC resolutions and for DAQ data is plotted below.

Each pulse presents a pre-trigger region of about 30 ns and 60 ns for OSC and DAQ system respectively, as Figure 5.1 shows. This latter consideration explains the minimum values of the following distributions. The DAQ waveforms show delta values always higher than OSC data.

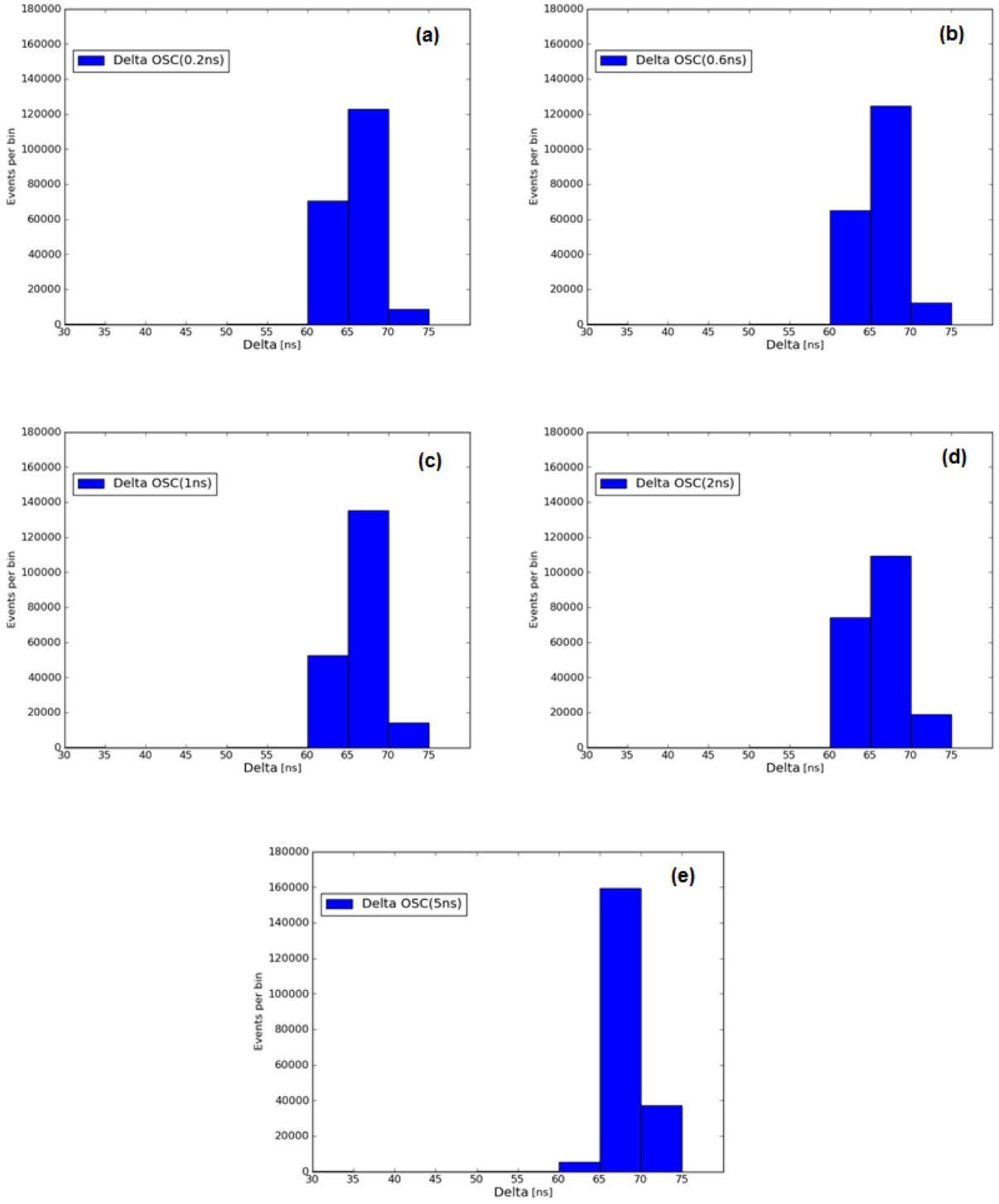

Figure 5.9. Delta distribution for OSC data for 0.2ns (a), 0.6ns (b), 1ns (c), 2ns (d) and 5ns (e) time resolutions.

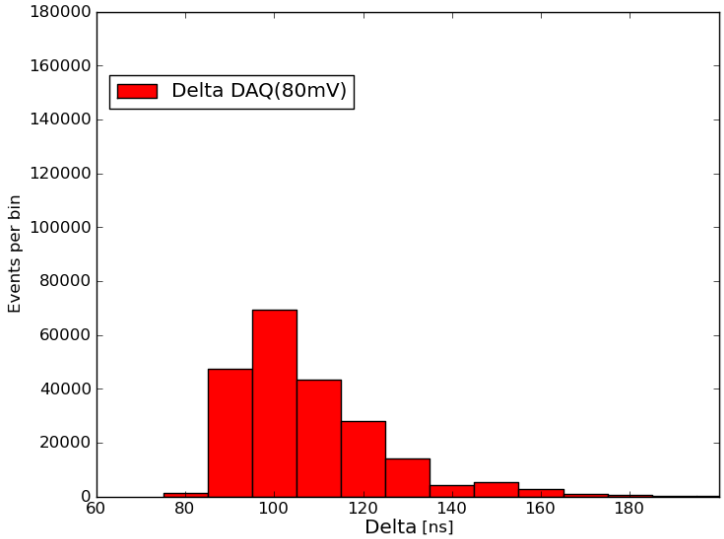

Figure 5.10. Delta distribution for DAQ(80 mV) data.

A value of delta around 64-65 ns has been considered as a good trade off. Waveform with delta under this limit have been counted and reported in table 5.1 with the corresponding residual waveforms, i.e. the new database size, for the whole set of OSC resolution.

L_{max} = 64 ns			
Resolution[ns]	**Dataset size**	**L_{max} [samples]**	**L_{max} [ns]**
0.2	166375	320	64
0.6	170948	106.67(107)	64.2
1	175833	64	64
2	187589	32	64
5	193724	13	65

Table 5.1. OSC dataset for L_{max}= 64 ns.

L_{max} = 65 ns			
Resolution[ns]	**Dataset size**	**L_{max} [samples]**	**L_{max} [ns]**
0.2	131562	325	65
0.6	129364	108.33(109)	65.4
1	142354	65	65
2	119710	32.5(33)	66
5	193724	13	65

Table 5.2. OSC dataset for L_{max}= 65 ns.

To give an example, for 0.2 ns, chosing L_{max} = 65 ns or L_{max} = 64 ns waveforms of the dataset vary from 131562 to 166375. In order to get a database constituted by waveforms with Delta>=L_{max} similar for al OSC time resolution L_{max} has been set to 64 ns.

In order to have the same statistics between OSC and DAQ dataset, we found appropriate to reduce the DAQ dataset to a comparable number of waveforms. Considering also that OSC waveforms are selected using a measurement threshold of 230 mV, different DAQ dataset are obtained varying the software threshold from the hardware 80 mV, as shown in table 5.3.

	OSC	DAQ			
	230 mV	80 mV	90 mV	100 mV	110mV
N° waveform dataset	162006	217192	198203	180405	165118

Table 5.3. DAQ dataset as a function of the software threshold implemented for the analysis.

Values higher than 110 mV will lead to a lower dataset than the one selected for OSC data, so they are not considered. L_{max} will be always bigger than 64 ns as shown in Figure 5.10.

If no restrictions are imposed, S can theoretically vary as:

$$1 \leq S \leq L_{max} - 1$$

and L as:

$$S + 1 \leq L \leq L_{max}$$

Defining S to vary to the end of the tail will be useless, it can be reasonable to consider S_{max} as the gate up to value where the pulse amplitude corresponds to 10% of the peak values. In order to verify the corresponding timing, the average pulse of the whole DAQ dataset has been considered, resulting in 30 ns after peak.

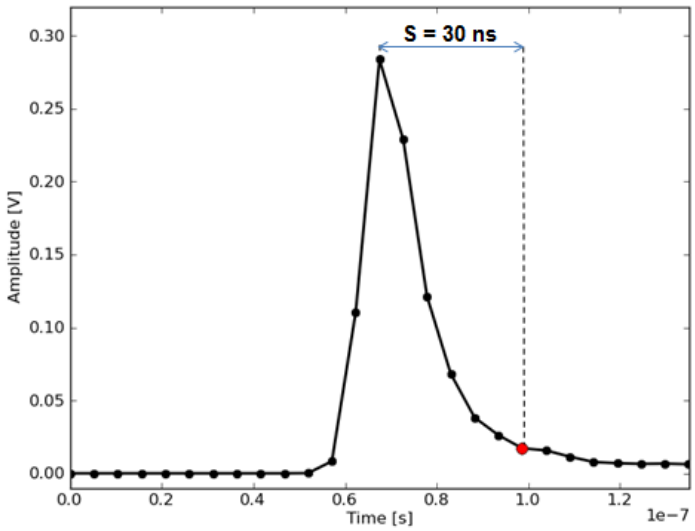

Figure 5.11. Determination of S_{max} from the DAQ dataset average pulse. The 10% of the pulse maximum is reached for 30 ns after the peak.

Considering that both S and L expressed in nanoseconds after peak, and now their restrictions, the two variable ranges are in this way related:

$$L = [S + 1, \dots, S_{max}\,]$$

$$S_{max} = 30\text{ns} \;\text{ and }\; L_{max} = 64\text{ns}$$

For each S-L combination the distribution S/L is obtained. The distribution features shapes which depends on whether the S-L gates used. The separation is obtained when S and L gates include portions of the waveform trailing edge which differs depending on the radiation.

2. The S/L distribution

An important parameter to set is the binning of the S/L distribution. Depending on the binning, the information contained in the S/L distribution can be highlighted or lost. For instance, too fine binning will show the very detailed structure of the distribution including statistical variations which magnitude could affect the analysis of its shape. On the other hand, a course binning would result in a rough shape which hides the effect of small changes induced by the choice of S and L when the distribution are compared. The binning impact on the S/L distribution has been studied considering 100 to 400 bins for S/L = (0, 1) (since S<L), as shown in Figure 5.12.

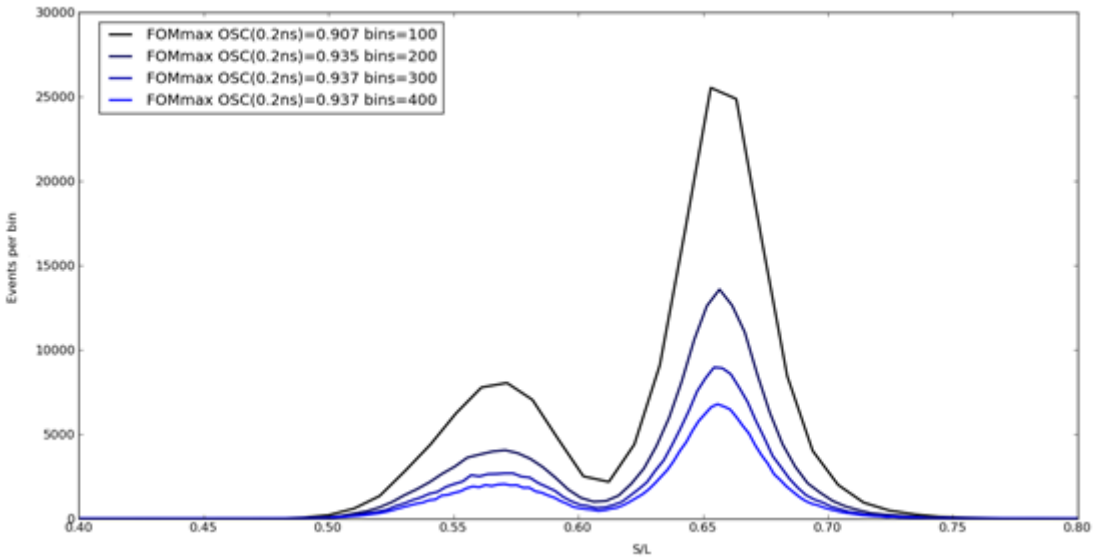

Figure 5.12. S_{op}/L_{op} distribution for 100 , 200, 300 and 400 bins. Using higher bins does not give rise to higher FoM for the optimal gates.

Moreover, considering the optimal gates for the oscilloscope data with different time resolutions, number of bins different from 200 does not give rise to higher FoM values. Furthermore, for 1 ns and 5 ns time resolutions bins lower than 200 do not allow n-γ discrimination for 1 ns and 5 ns time resolutions.

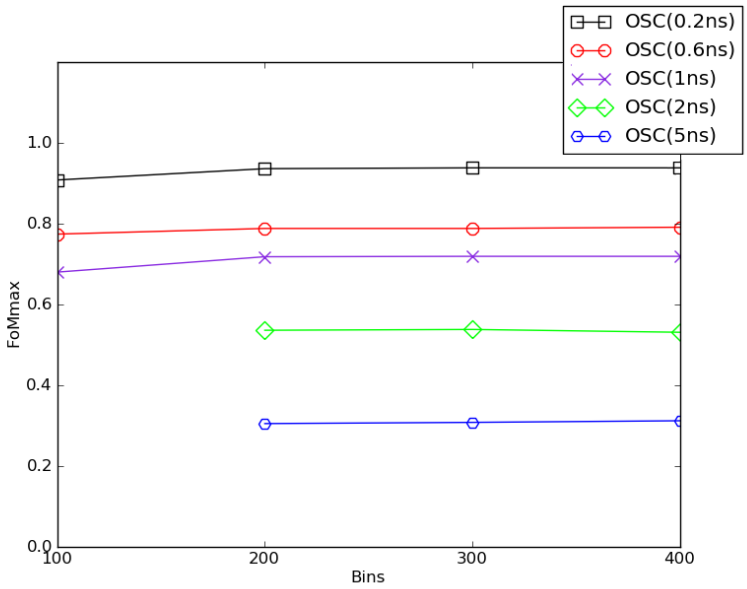

Figure 5.13. Different OSC time resolutions FoM_{max} values for 100 , 200, 300 and 400 bins. Bins higher than 200 does not give rise to higher FoM values.

As a trade-off between the amount of waveforms in the database, the convergence of the fitting routine used in the analysis and the detail expected in the n-γ discrimination for different S-L gates, the binning over 200 was chosen.

3. Determination of the FoM

When the S-L gate combination allows for n-γ separation, the S/L distribution is *double humped*. Due to the different light emission induced in the scintillator, neutrons features low S/L values, i.e., the left hand side lobe of the S/L distribution. Radiation events with small energy deposition in the scintillator, either neutrons or gammas, will give rise to pulses with S/L ratio in the overlapping region between the two n and γ lobes. The optimal S-L gate combination maximize the n-γ discrimination resulting in the smallest overlapping region.

The algorithm implemented in the pulse shape analysis calculates the S/L distribution, analyze it determining the FoM for each S-L gate combination. In order to strengthen the analysis algorithm with respect to this glitches avoiding in the shape, the S/L distribution has been smoothed.

The simplest form of smoothing, which is the one we used, is the "moving average" that basically replaces each value in the bin with the average of neighboring bins. Figure 5.14 shows in detail the comparison between the calculated S/L distribution and the smoothed one. The region between the neutron and gamma maximum will be thus identified without ambiguities. The input values to the FoM in term of maximum neutron and gamma lobes, and the minimum between maxima for a S/L histogram where glitchs are evident.

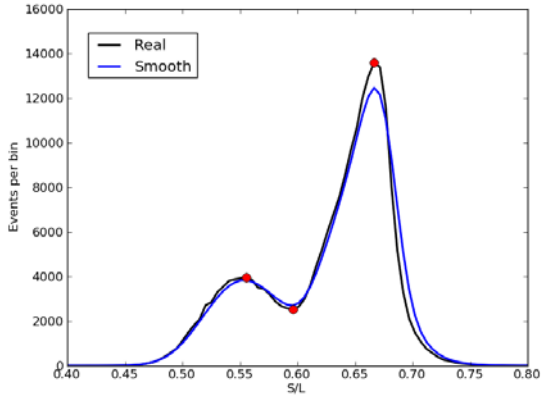

Figure 5.14. Calculated and smoothed S/L distribution histogram. Smoothing strengthen the analysis avoiding the glitches due to statistical variations.

These step of analysis have been set comparing initially the OSC(0.2 ns) and DAQ(5 ns) databases.

Oscilloscope data

All the waveforms collected with the oscilloscope have the same length of 100 ns, i.e., 500 samples. Due to the high sampling frequency, a study has been pursued to investigate the effect of the time resolution on the n-γ discrimination. The oscilloscope data has been downsampled up to the time resolution of the KN3 DAQ (5 ns) as summarized in the following table:

Resolution [ns]	Samples
0.2	500
0.6	166
1	100
2	50
5	20

Table 5.4. Time resolutions and samples considered in the analysis of the oscilloscope waveforms

The downsampling of the oscilloscope waveforms is obtained extracting one point each 3, 5, 10 and 25 samples in order to obtain respectively a resolution of 0.6, 1, 2 and 5ns.

Figure 5.15 shows the waveforms corresponding to 0.6 ns and 5 ns time sampling from the original one.

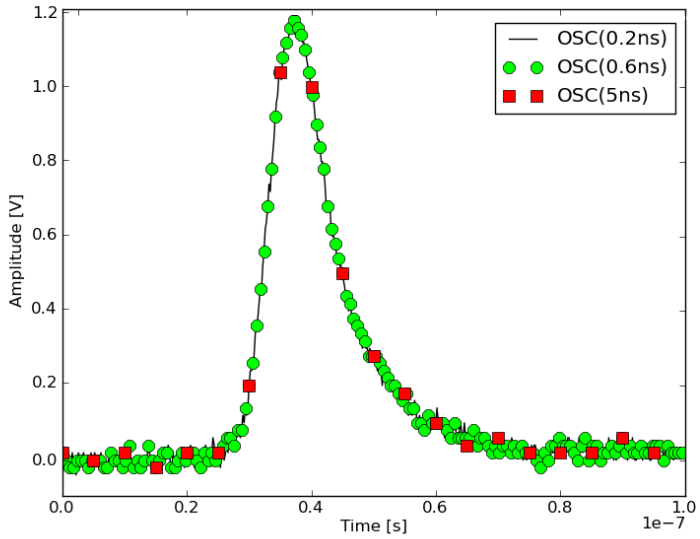

Figure 5.15. Waveforms of OSC(0.6 ns) (green dots) and OSC(5 ns) (red squares) time resolution obtained from oscilloscope waveform sampled at 5 GHz.

The investigation aims to demonstrate the advantage of a digital acquisition system capable of higher sampling rate of the signal pulse shapes induced by the radiation events in the detector.

The short and long gate limits S_{max} and L_{max} used in this study depend on the time resolution and are summarized in Table 5.5.

Resolution[ns]	S_{max} [ns]	L_{max} [ns]	S_{max} [samples]	L_{max} [samples]
0.2	30	64	150	320
0.6	30	64.2	50	107
1	30	64	30	64
2	30	64	15	32
5	30	65	6	13

Table 5.5. Short and long gate maxima limits, in ns and samples.

Figures 5.16 represents the results in terms of FoM phase space for all S-L gate combinations for the OSC(0.2ns) dataset according to Fit N method.

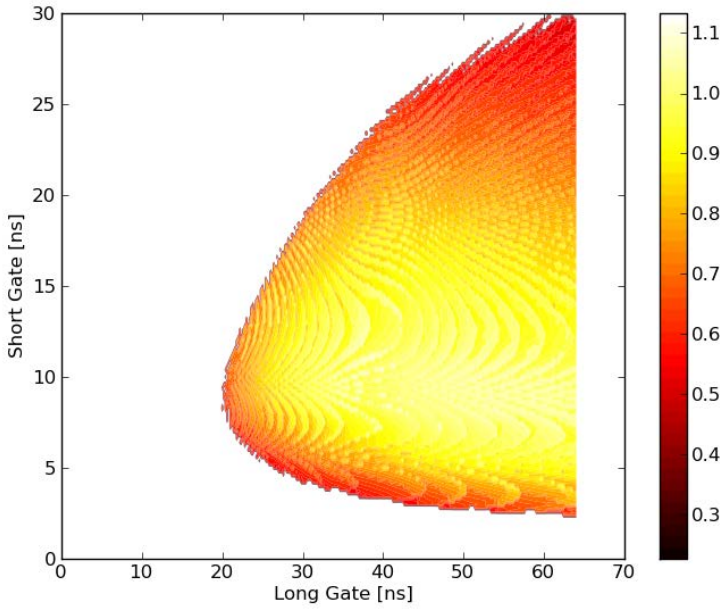

Figure 5.16. Fit N FoM contour plot for OSC(0.2ns) dataset.

Different regions can be recognized in the figure. The white region of the contour plot features no events. This is due to the assumption made for the calculation of the FoM which is determined only if the S/L distribution is double humped, i.e., a local minimum exists between the neutron and gamma lobes. This results in the sharp boarder of the contour plot.

The waveforms start to be identified as neutron or γ interactions in the scintillator as soon as S and L gates include portions of the waveforms trailing edges. A first region with FoM < 0.9 corresponds both to a small portion of the waveform immediately after the peak [S < 10, L > 20 ns] and to increased portion of the trailing edge [S > 20, L > 40 ns]. These areas do not improve the n-γ discrimination. The region with FoM > 0.9 correspond to the yellow areas which give rise to well separate lobes. Oscillations in FoM values are due to the method to calculate $FWHM_\gamma$. This relates to the range of x_γ corresponding to $y_\gamma \geq \frac{y_{\gamma_{peak}}}{2}$. For different gate combinations, the $FWHM_\gamma$ varies slightly giving rise to the pattern of FoM values displayed in Figure 5.16. This can be reduced fitting the gamma lobe, thus using in the FoM calculation the σ_γ output of the fit. In fact, Fit NG contour plot looks more homogeneous than the previous one, as Figure 5.17 shows.

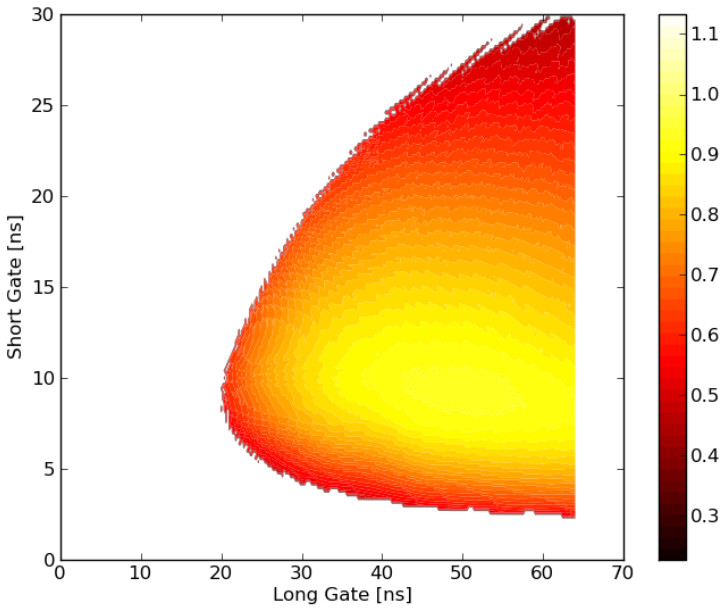

Figure 5.17. Fit NG FoM contour plot for OSC(0.2 ns) dataset.

Similarly to the previous figure, two regions can be individuated in the contour plot with smoothed boundaries. FoM values are also on average lower than the previous due to the gamma fit. A region with FoM < 0.9 wider than the one in Figure 5.16 and the yellow region of FoM > 0.9 are better defined.

For the third method of analysis, Fit All, if the lobe are well separated the results are similar to Fit NG, as shown in Figure 5.18.

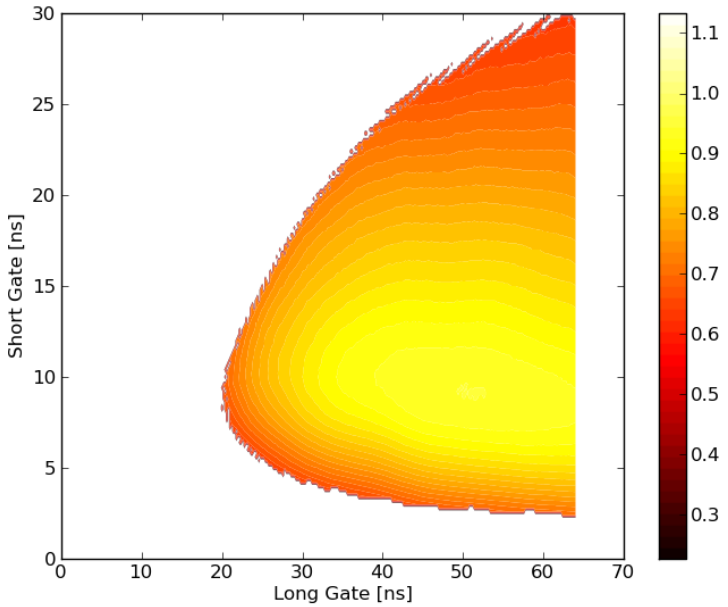

Figure 5.18. Fit All FoM contour plot for OSC(0.2 ns) dataset.

In this case the region with FoM > 0.9 is wider with respect to Figure 5.17 and the contour plot features lower gradients. If the neutron and gamma separation is good, the fit results almost identical.

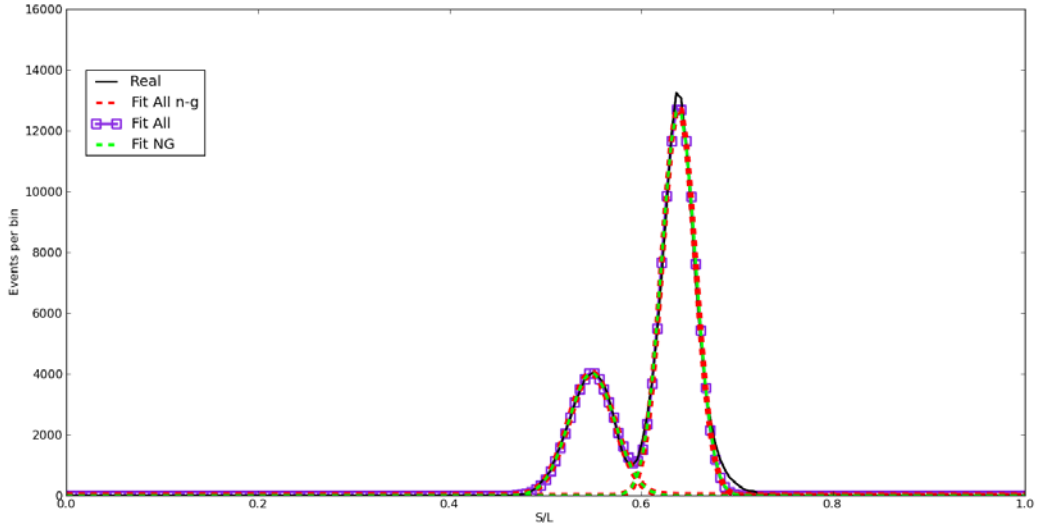

Figure 5.19. Comparison of Fit NG and Fit All for FoM > 0.9 gate combination. The fits are almost identical.

In the worse cases instead the two fitting methods provide slightly different results.

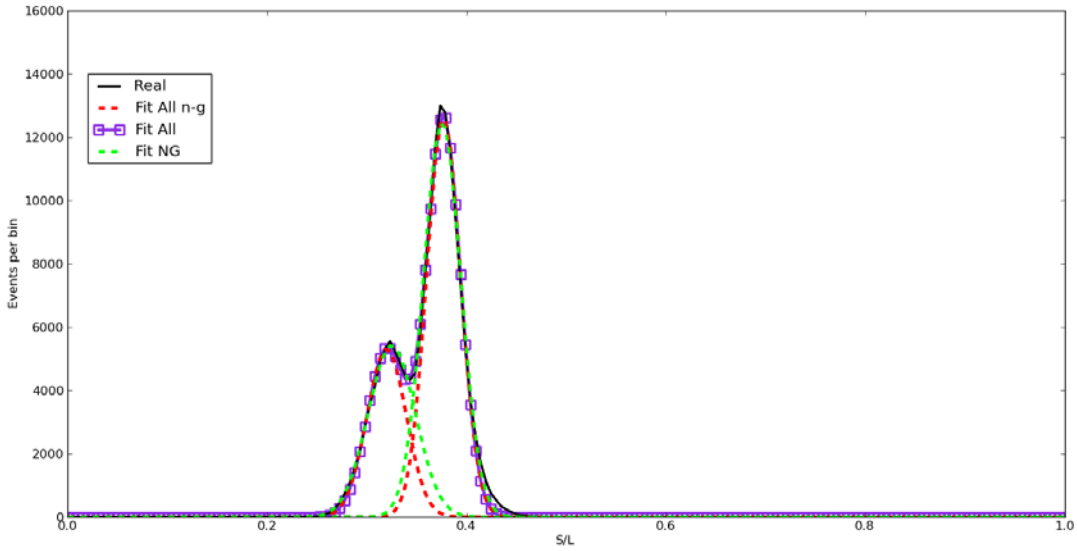

Figure 5.20. Comparison of Fit NG and Fit All for FoM < 0.9 gate combination.

The variation of FoM calculated with Fit All are smaller since the convergence of the fitting function, sum of two Gaussians, is more robust.

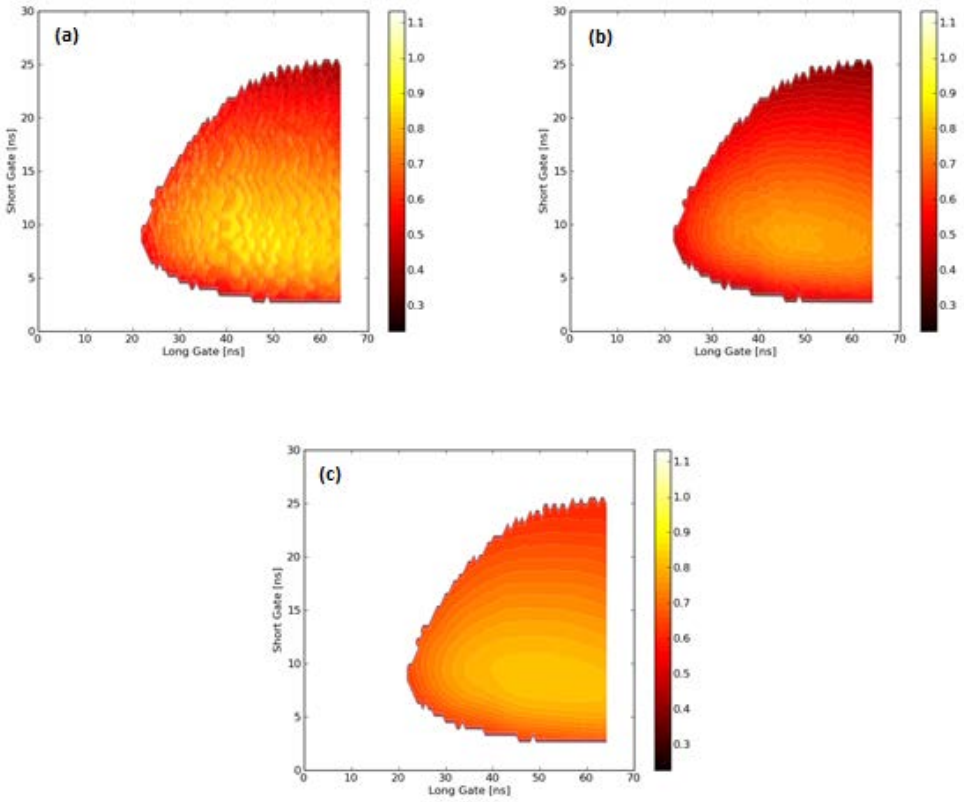

Figure 5.21. Comparison of FoM contour plots obtained for OSC(0.6 ns) database using Fit N (a), Fit NG (b) and Fit All (c).

For 0.6 ns time resolution FoM maximum is 0.9 for Fit N method of analysis (Figure 5.21 (a)). The S/L distributions feature lower separation of the neutron and gamma lobes and they converge to S ≤ 25 ns and L ≥ 22 ns. This is different with respect to OSC(0.2 ns) (S ≤ 30 ns and L ≥ 20 ns). Comparing Fit NG contour plot between 0.2 and 0.6 ns (Figure 5.21(b)), FoM is set on lower values. This fact can be justified considering that pulses processed are less accurately defined with a lower resolution, giving rise to a worse separation in S/L distribution. Oscillations in FoM values are due to the gamma lobe analysis method as for 0.2 ns resolution. Variation are reduced considering Fit NG FoM contour plot and even more Fit All FoM phase space.

Fit NG contour plot holds FoM values from 0 to 0.8. The region with FoM > 0.7 correspond to gates S = [5, 14] ns and L = [30, 64.2] ns which give rise to well separate lobes In this region FoM maximum values are located in the area limited by S = [7, 10] ns and L = [42, 52] ns. A more homogeneous contour plot is obtained using Fit All method is displayed in Figure 5.21 (c).

In Fit All contour plot FoM varies up to a maximum 0.8. A first region with FoM within 0.6 and 0.75 con be identified for S = [3, 5] ns and S = [16, 27] ns. The second region with FoM > 0.75 is localized for S = [16, 27] ns L = [30, 64] ns. In this area the maximum FoM values are identified in the region limited by S = [7, 11] ns and L = [42, 64] ns.

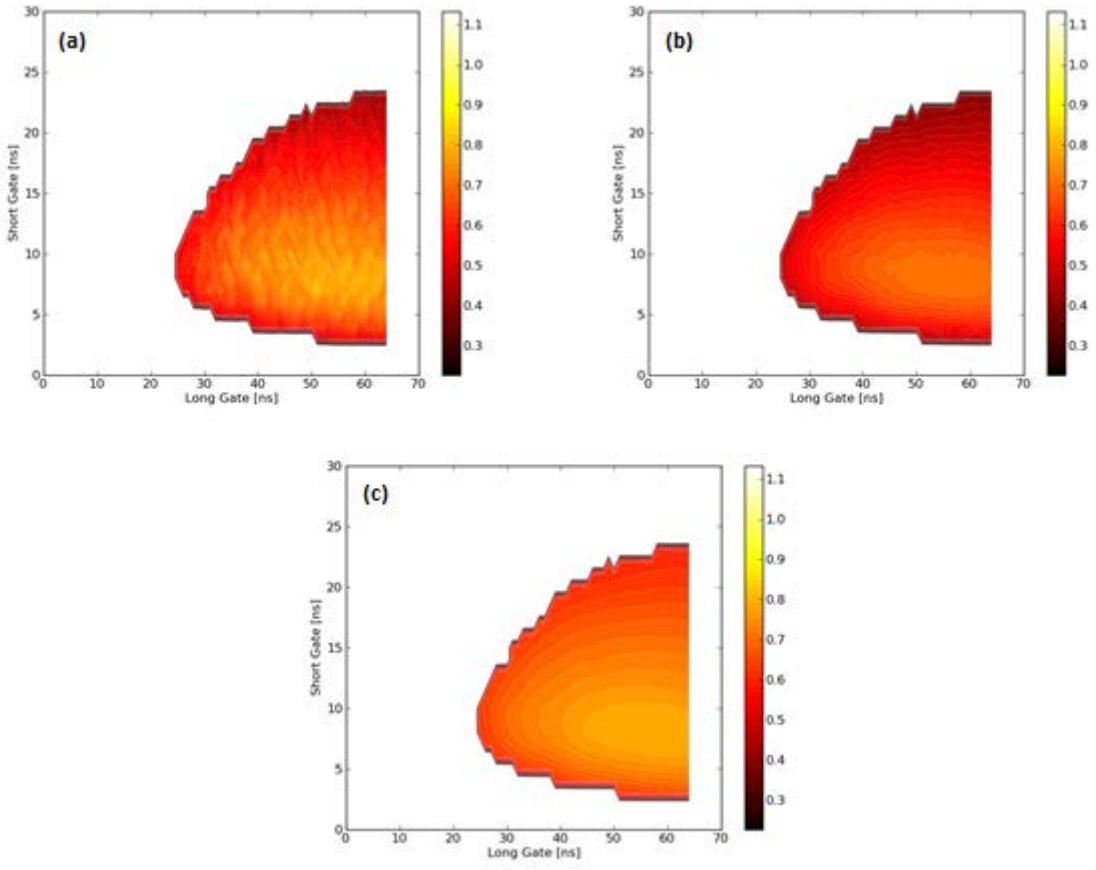

Figure 5.22. Comparison of FoM contour plots obtained for OSC(1 ns) database using Fit N (a), Fit NG (b) and Fit All (c).

Fit N contour plot is defined within S ≤ 23 ns and L ≥ 25 ns with FoM ≤ 0.8. As observed before, Fit All results in a FoM distribution smoothed with the region of maximum FoM values limited by S = [6, 11] ns and L = [45, 64] ns.

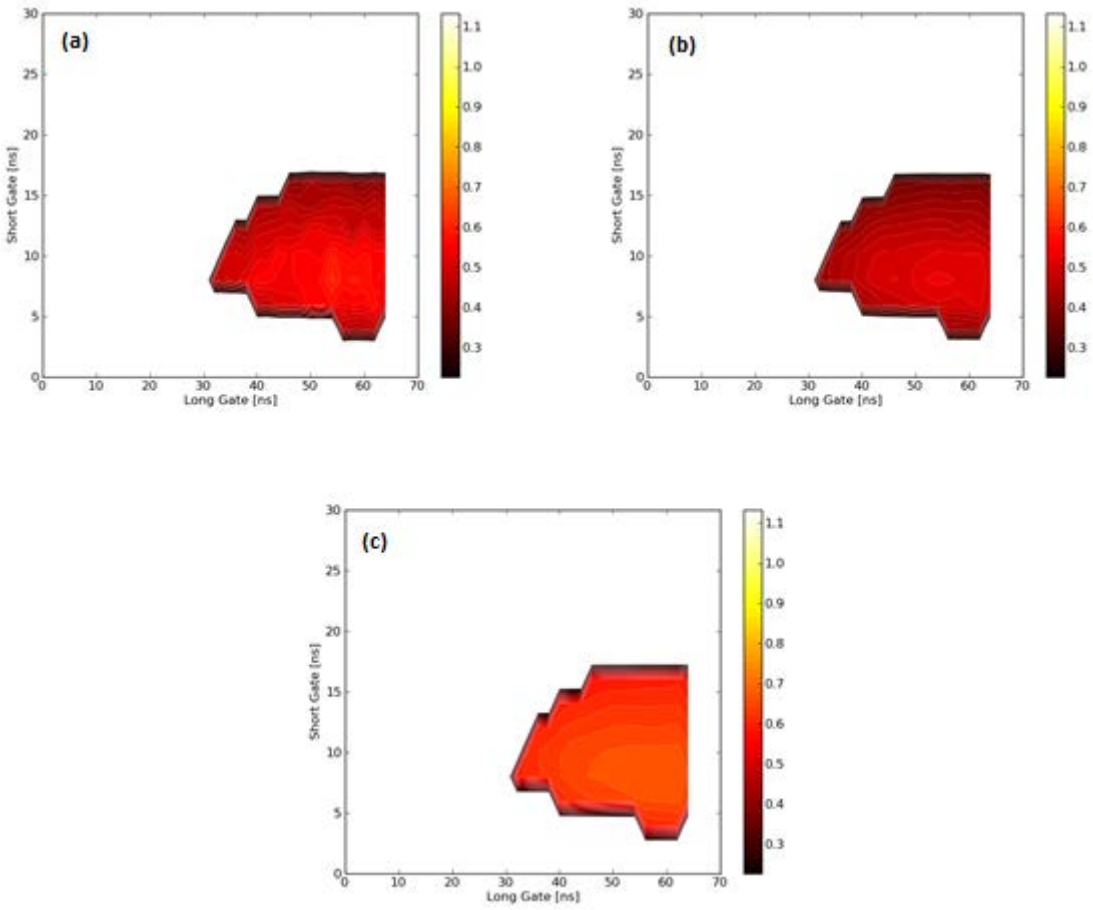

Figure 5.23. Comparison of FoM contour plots obtained for OSC(2 ns) database using Fit N (a), Fit NG (b) and Fit All (c).

For OSC(2 ns) database the FoM distribution is within S = [4, 17] ns and L = [30, 64] ns. The maximum value reached is 0.6. The contour plots shows quite marked boarders and little variation of the FoM.

In Fit N, the region of low FoMs is defined by S =[3, 5] ns and S =[13, 17] ns determined FoM < 0.55. S = [5, 13] ns and L = [40, 64] ns defines the region of FoM > 0.55. Inside this region FoM maximum values area is defined by S = [6, 10] ns and L = [51, 60] ns.

In Fit NG, FoM values vary up to 0.52. The region of low FoMs is defined by S =[3, 6] ns and S =[12,17] ns determined FoM < 0.52. S = [6, 12] ns and L = [40, 64] ns defines the region of FoM > 0.55, in which FoM maximum values are confined in S = [7, 9] ns and L = [52, 54] ns.

In Fit All the low FoM values region is concentrated in a small stripe along the border, only a small region where FoM quckly varies from 0.5 to 0.60.

As just presented, the lower is the resolution, the smaller is the overall FoM phase space where separation is obtained. Figure 5.24 displays results for OSC(5 ns) database. Only few S-L combinations result in S/L distribution of FoM higher than zero for only Fit N and Fit NG. Fit NG method does not converge here due to the weak neutron and gamma lobes for 5 ns resolution which does not lead to a well double humped S/L distribution.

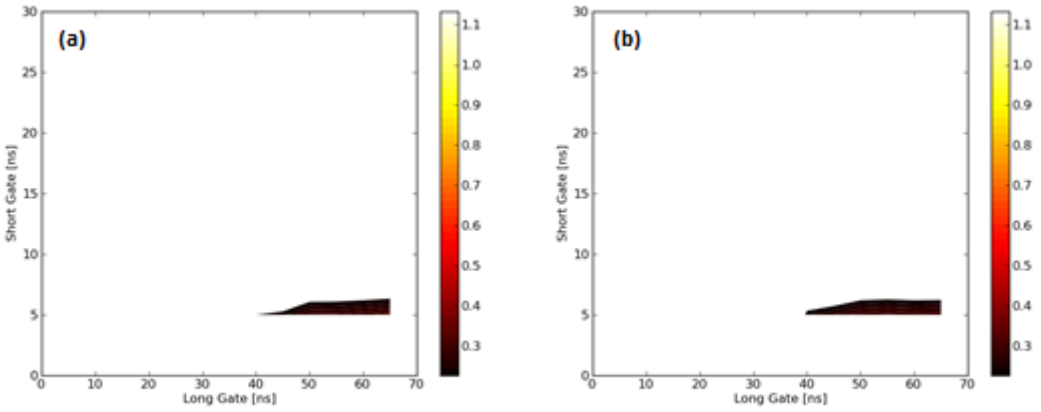

Figure 5.24. Comparison of FoM contour plots obtained for OSC(5 ns) database using Fit N (a), Fit NG (b).

Here only S = [5, 7] ns and L = [40, 65] ns gate combinations give rise to a FoM up to 0.3.

Figure 5.25 displays the contour plot obtained for OSC(5 ns) dataset, considering only FoM ≤ 0.3.

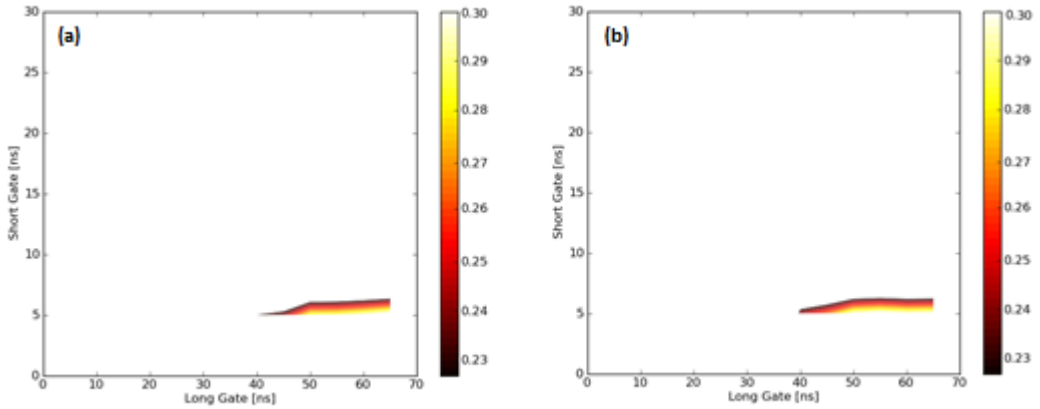

Figure 5.25. As Figure 5.24 but for FoM ≤ 3.

Comparison of the FoM contour plots for different resolutions shows that the higher is the resolution the wider is the region where neutrons can be discriminated from gammas. Using combinations with gates S ≥ 15 ns ans L ≥ 30 ns does not add additional information (see Figure 5.11). In this case S reaches trailing edge amplitude up to 30% of the pulse maximum which already includes information on the slow decay constant as L gate.

For very long L gates, the information brought about is minor due to the pulse amplitude in this region comparable to the noise level. The uncertainties featuring these pulse amplitude values is comparable to the amplitude values themselves and results in a S/L distribution smeared out [13].

Figure 5.26-28 display horizontal (S = 10 ns) and vertical (L = 55 ns) profiles of the FoM contour plots of the OSC database with different time resolutions for the three methods of analysis.

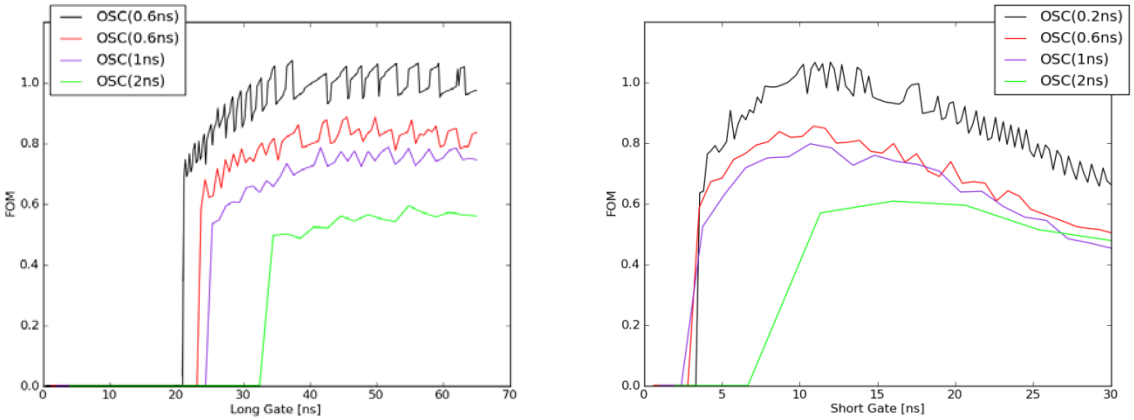

Figure 5.26. Fit N FoM variations for a fixed L(55ns) and S(10ns).

The oscillations for OSC(0.2ns) and Fit N seems related to odd-even number of samples considered in the S and L gates. This feature disappears fitting the lobe of the S/L distribution.

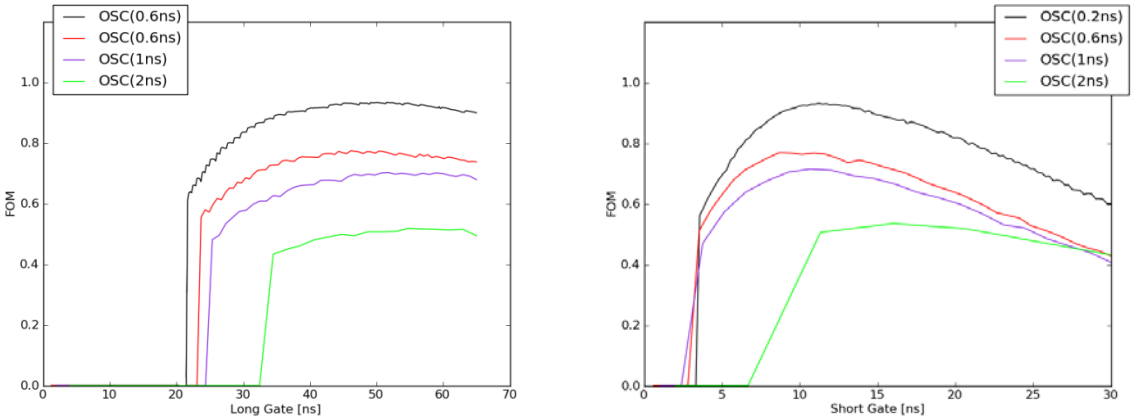

Figure 5.27. Fit NG FoM variations for a fixed L(55ns) and S(10ns).

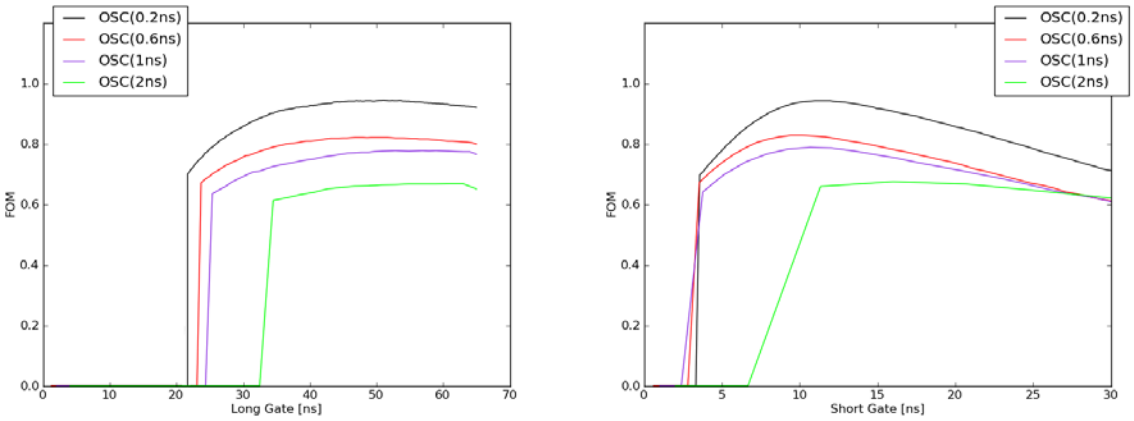

Figure 5.28. Fit All FoM variations for a fixed L(55ns) and S(10ns).

Table 5.6 summarizes the optimal S-L gate combinations and the maximum FoM values for the oscilloscope data analyzed with different time resolutions for the three methods. To verify the goodness of the optimal S-L gate combination, the parameter R, i.e. the γ/n ratio of the events within the lobes of the S_{op}/L_{op} distributions, has been calculated. For this, the real curve has been considered. The result depends on both the time resolution and the method. It has been also considered the possibility of calculate R using the minimum of the total fit and the total fit curve as well, respectively for Fit NG and for Fit All. When found, the results vary from 2.7 up to 2.1 as shown in the table is in accordance with the expected ^{241}Am/^{9}Be branching ratio.

		OSC (Delta pulselength-peak>=64ns)				
		Time resolution				
		0.2ns	0.6ns	1 ns	2 ns	5 ns
	N° waveform dataset	162006	162006	162006	162006	162006
R (minimun real distribution)	Fit N	2.54	2.53	2.41	2.47	2.14
	Fit NG	2.53	2.53	2.45	2.47	2.49
	Fit All	2.48	2.44	2.36	2.22	-
R (minimun fit sum)	Fit NG	2.47	2.66	2.55	-	-
	Fit All	2.45	2.36	2.49	2.48	-
FOM_{max}	Fit N	1.12	0.92	0.83	0.61	0.31
	Fit NG	0.94	0.79	0.72	0.54	0.30
	Fit All	0.95	0.83	0.79	0.68	-
FOM_{max} variation	Fit N		18%	26%	46%	72%
	Fit NG		16%	23%	43%	67%
	Fit All		12%	17%	28%	-
FOM_{max} average variation			**15%**	**22%**	**39%**	**70%**

Table 5.6. OSC dataset R γ/n ratio and FoM_{max} for different time resolutions.

Where FOM_{max} variation is definited:

$$FOM_{max}variation\ \% = \frac{FOM_{max_{0.2\ ns}} - FOM_{max_{i\ ns}}}{FOM_{max_{0.2\ ns}}} \cdot 100, \quad i = [0.6, 1, 2, 5]$$

Since the comparison of the different time resolutions is consistent only if comparable events are considered, distributions have been integrated in order to have the same number of events in each case. Values for each single method and resolution are reported in the first rows of Table 5.6 and they are in any case similar. Waveforms that are not considered in the distributions represent pile up events with a large amount of the tail set under zero.

Figure from 5.29 represents the results in terms of R phase space for all S-L gate combinations for 0.2 ns time resolution.

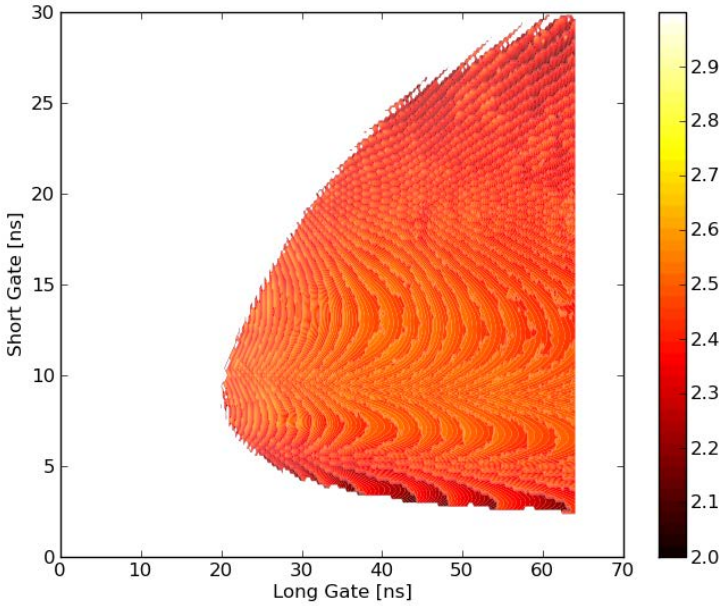

Figure 5.29. R contour plot for the OSC(0.2ns) dataset.

The white region features no events and the γ/n ratio cannot be calculated. R is always in the range expected from the branching ratio with a variation within 2.4 and 2.8.

The following scatter plots illustrate the correlation of FoM with R for the three methods of analysis and time resolution of OSC dataset (Fig.5.30).

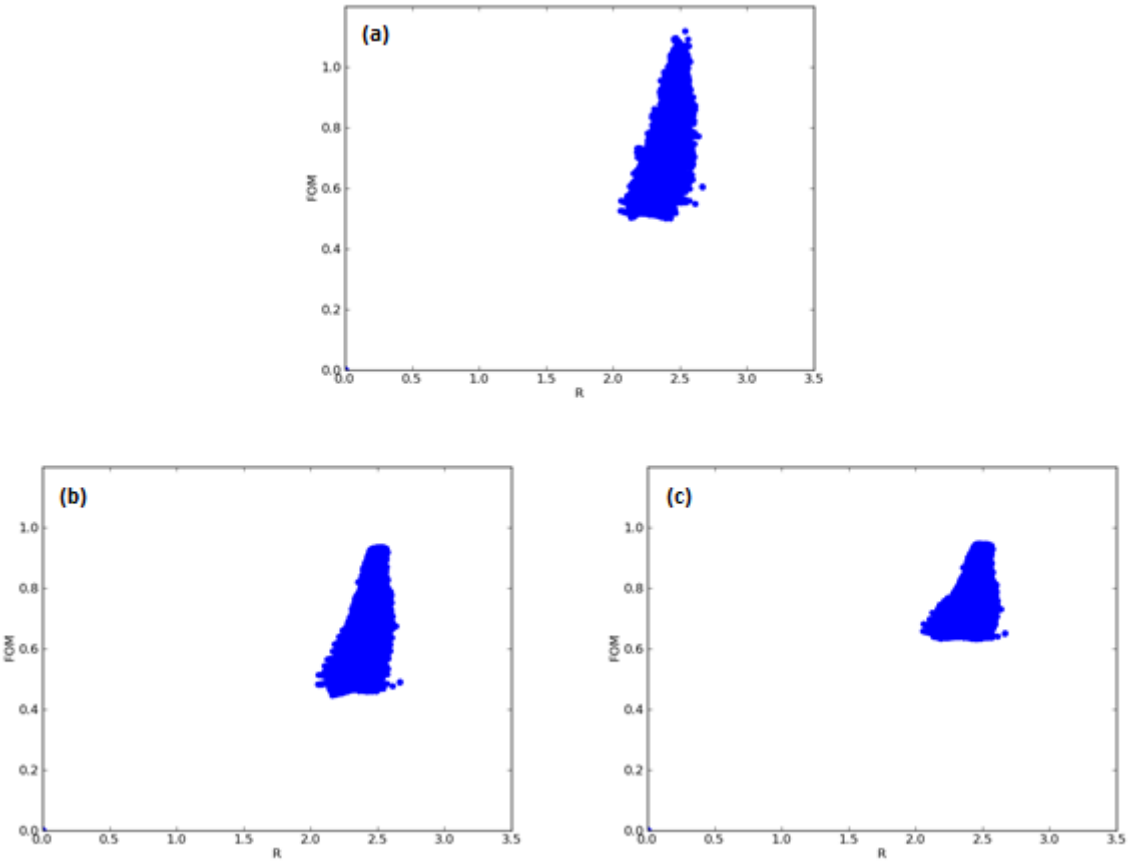

Figure 5.30. FoM vs R scatterplots for the OSC(0.2ns). Variation of FoM and R is gradually reduced considering Fit N, Fit NG and Fit All method of analysis.

For the three method considered, R values are always in the range expected and the FoM fluctuations are gradually reduced considering Fit N, Fit NG and Fit All method of analysis. S/L gate combinations which give rise to a double humped distribution are 21735 for the three methods. Fit N results in variations of FoM within 0.5 and 1.12, Fit NG within 0.5 and 0.94 and where FoM is concentrated within 0.65 and 0.95 for Fit All. The ranges corresponds to 124%, 88% and 46% respectively. As reported in table 5.6 FoM_{max} corresponds to R values equal to 2.5, respectively for Fit N, Fit NG and Fit All.

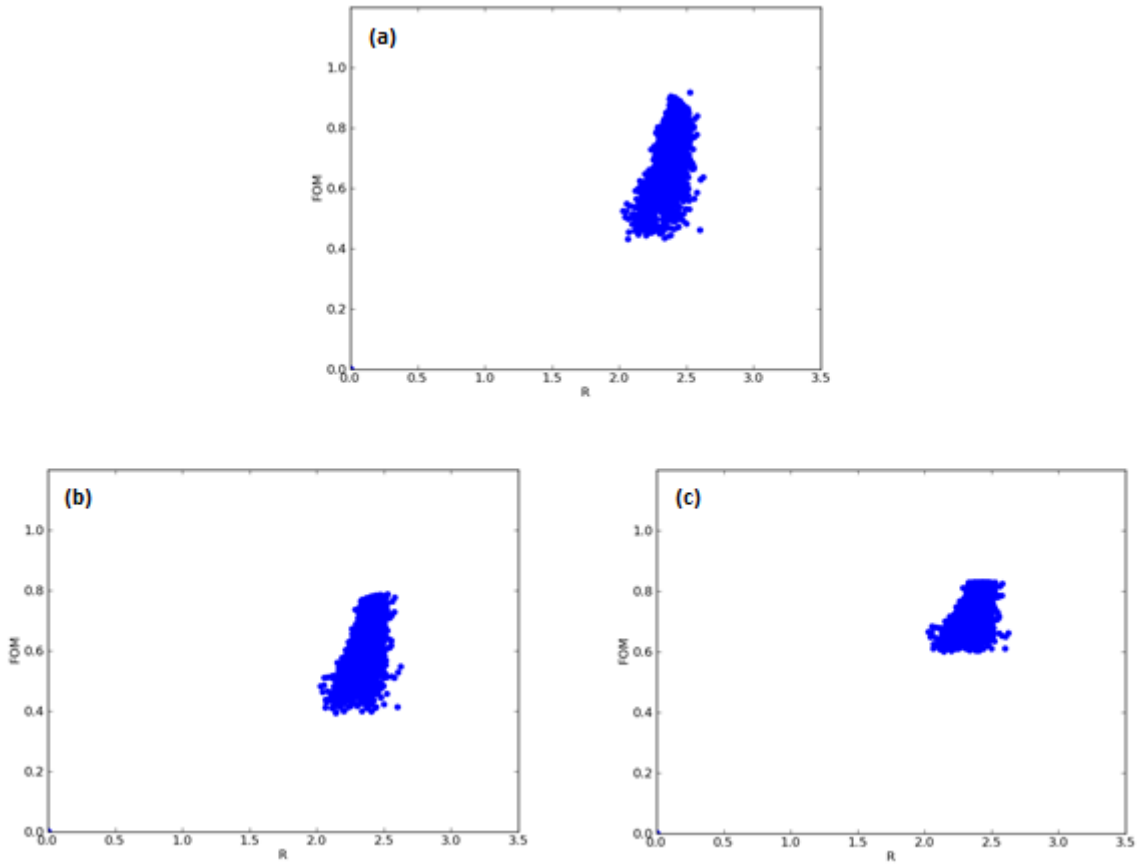

Figure 5.31. As Figure 5.30 but for OSC(0.6ns) dataset.

The lower FoM variation passing from Fit N to Fit NG is evident also for 0.6 ns. S-L combinations which give rise to separate lobes distributions are 2036 for the three methods of analysis. FoM varies from 0.41 to 0.92 (124%) for Fit N, from 0.4 to 0.78 (95%) for Fit NG and within 0.6 and 0.83 (38%) for Fit All. FoM values correspond to R values equal to 2.5, 2.5 and 2.4 respectively.

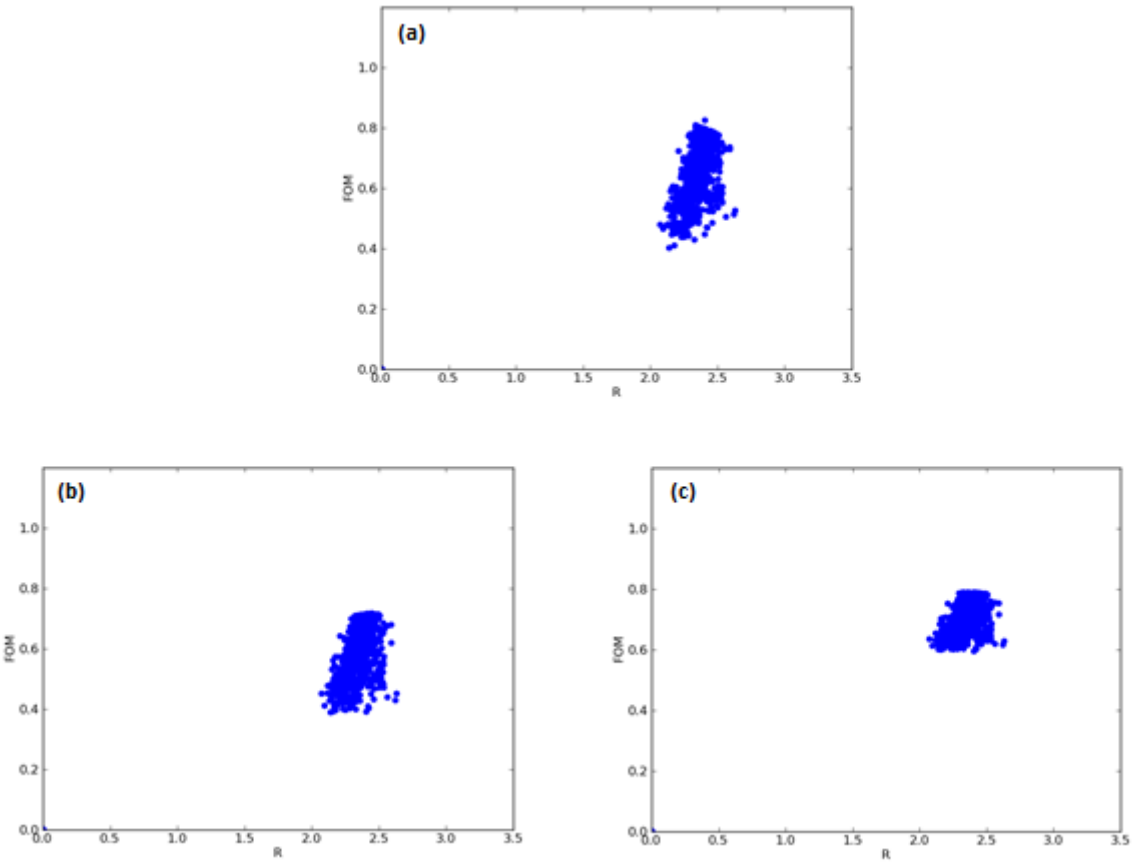

Figure 5.32. As Figure 5.30 but for OSC(1ns) dataset.

Here FoM features variations of 113%, 83% and 32% for S/L gate combinations of 629. FoM_{max} values corresponds to R values equal to 2.4, 2.5 and 2.4 respectively.

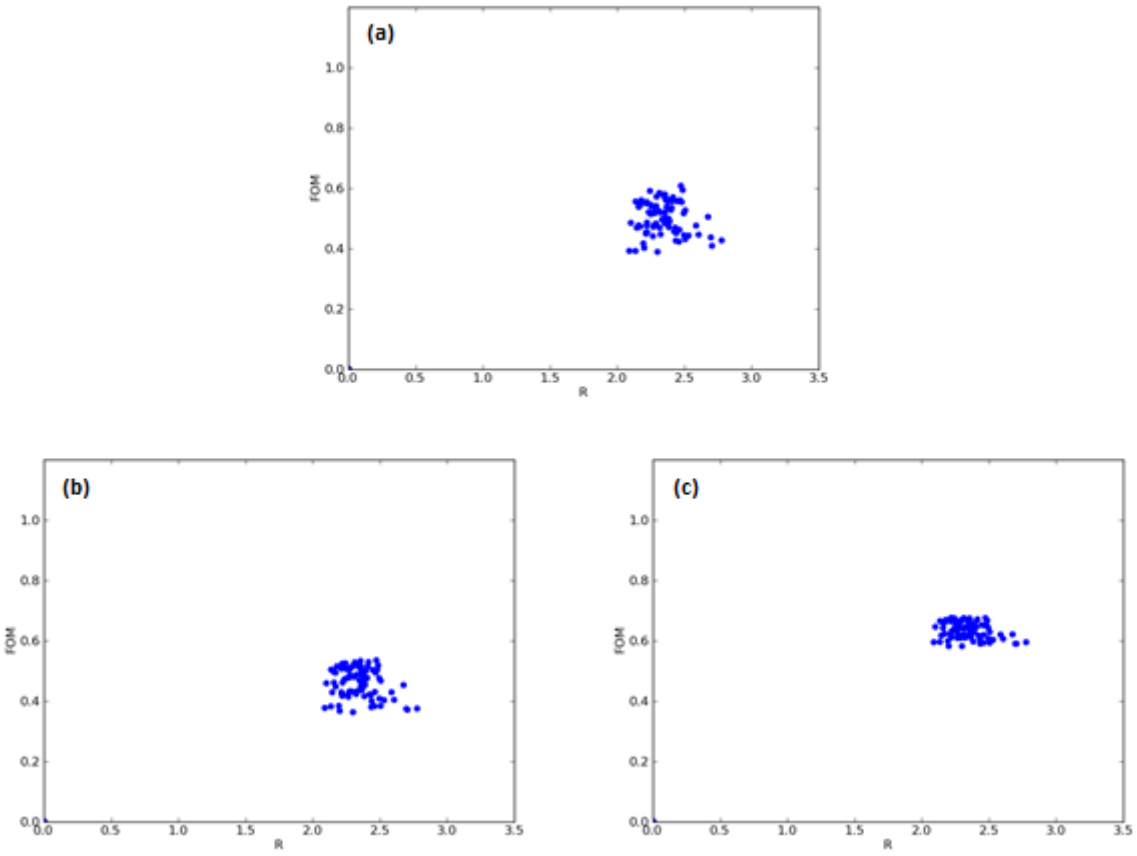

Figure 5.33. As Figure 5.30 but for OSC(2ns) dataset.

FoM is calculated for 88 S/L contributions and features variations of 50%, 42% and 15% with R equal to 2.5, 2.5 and 2.2, respectively for Fit N, Fit NG and Fit All.

To observe is the reduction of S-L gate combinations that result in a double humped S/L distribution useful for FoM determination.

This is also true for OSC(5ns) database (Figure 5.33) which displays 6 S/L gate combinations.

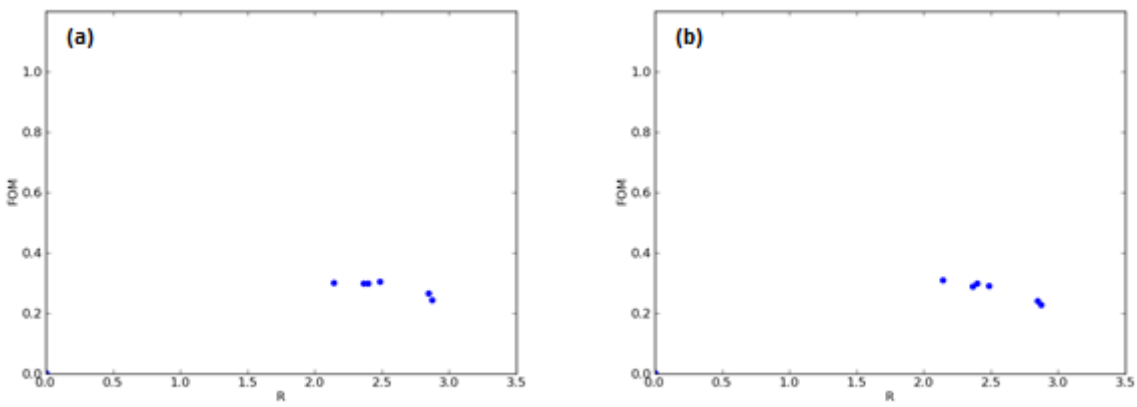

Figure 5.34. As Figure 5.30 but for OSC(5ns) dataset.

Here only Fit N and Fit NG were performed. FoM varies within 0.21 to 0.31 for Fit N, and from 0.2 to 0.30 for Fit NG. R results values equal to 2.1 and 2.5 respectively.

If R is calculated considering the sum of the two lobe fit for NG (Fit NG Sum) shown in Figure 5.35, it necessary to consider that it could give a minimum position different if compared with the real curve one. Furthermore, for 2 ns and 5 ns Fit NG Sum minimum does not exist (Figure 5.35(d) and (e)).

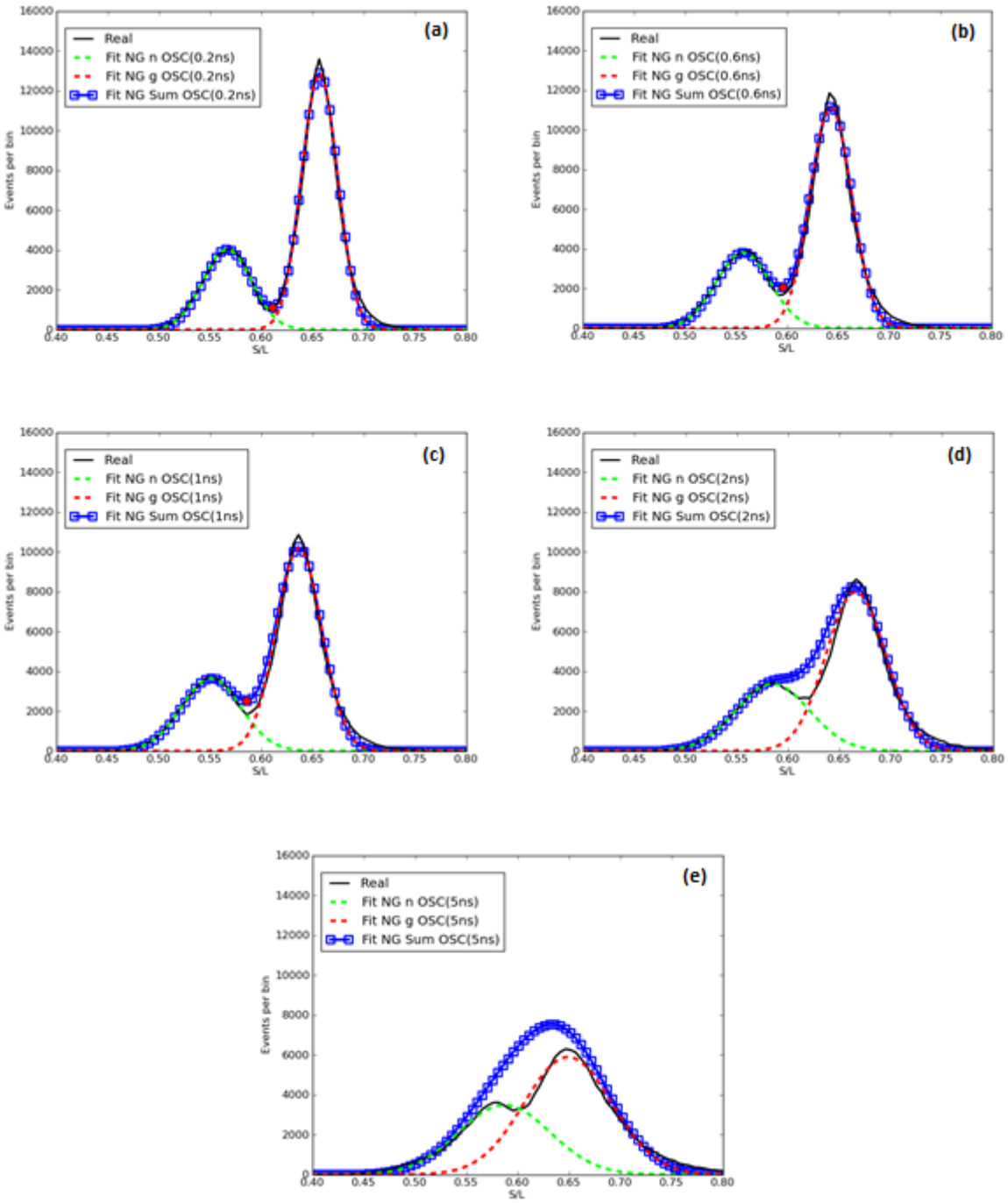

Figure 5.35. Fit NG Sum fit for the different OSC time resolutions. The minimum position for the fit corresponds to the one of the real curve for 0.2, 0.6 and 1 ns; R cannot be calculated for 2 and 5 ns time resolutions.

Since Fit All method aims at reproducing the real curve as of a double Gaussian fit, such that it is more similar to the real curve than the Fit NG (Figure 5.36). The position of the minimum from Fit All is correct for OSC(0.2ns) S/L optimal distribution.

Table 5.6 does not report values for OSC(5ns). Since the separation in S/L distribution is always weak for 5 ns resolution the resulting fit does not converge as shown in Figure 5.36(e).

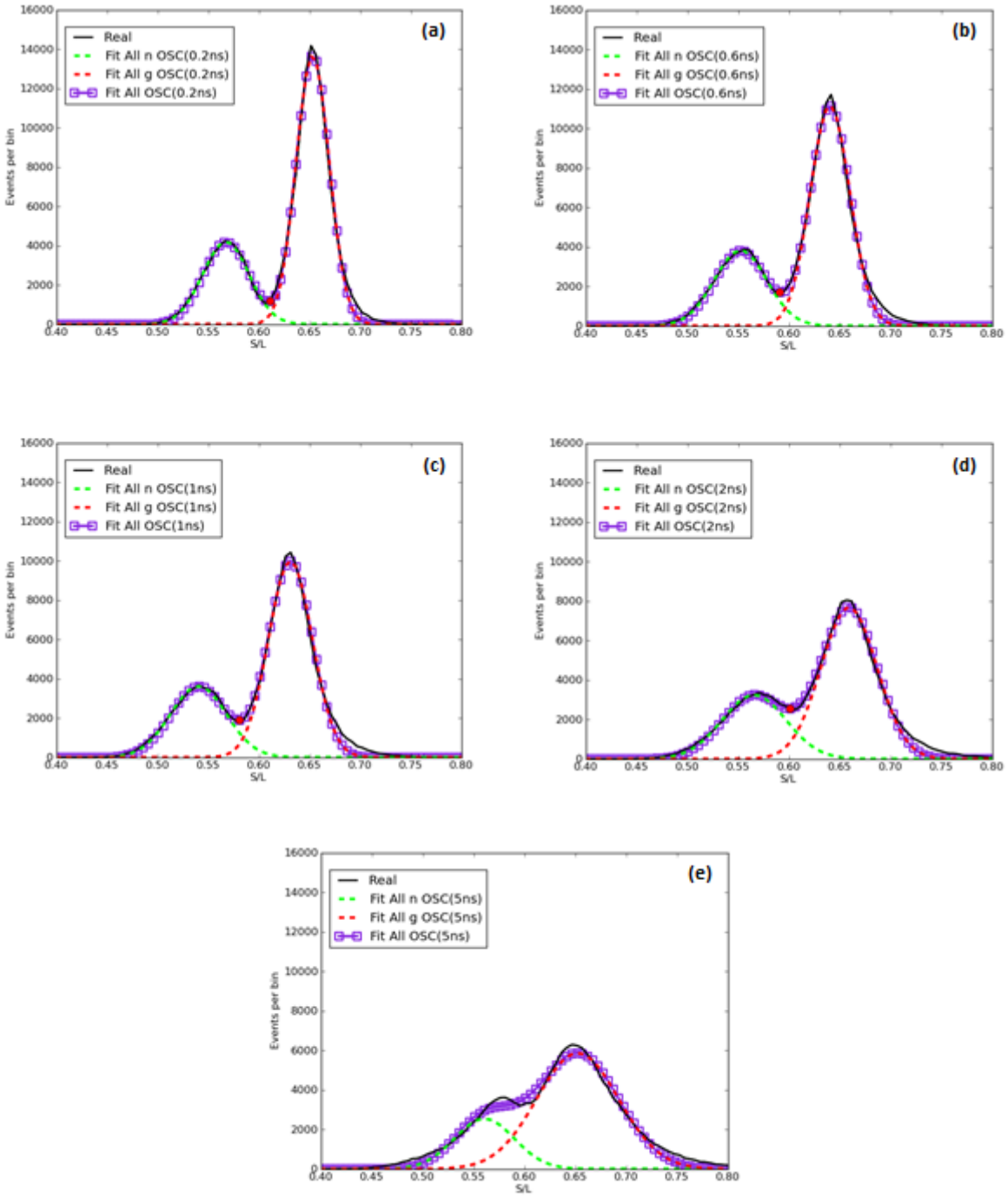

Figure 5.36. As Figure 5.35 for Fit All method.

It is clear from the Gaussian fits that in the region of the minimum of the S/L distribution, events due to neutron interaction fall into the gamma lobe of the distribution (n_γ) and viceversa (γ_n).

Using the S_{op}/L_{op} distribution, the contamination of neutron and gamma events has been assessed. Table 5.7 summarizes the results.

		OSC (Delta pulselength-peak>=64ns)				
		Time resolution				
		0.2ns	0.6ns	1 ns	2 ns	5 ns
	N° waveform dataset	162006	162006	162006	162006	162006
S_{op}/L_{op}	Fit neutr	8.6/43.6	8.4/48	7/51	8/54	5/65
	Fit Gauss1	9.2/49.6	8.4/48	8/51	8/54	5/55
	Fit Gauss2	8.8/51.4	8.4/49.8	8/56	8/62	-
n_γ [events]	Fit NG	2236	4854	6932	15329	34172
	Fit All	2146	3101	5234	7566	-
γ_n [events]	Fit NG	572	1303	1651	4073	14903
	Fit All	473	999	984	2302	-

Table 5.7. OSC dataset optimal S_{op}/L_{op} gate combination with their neutron and gamma events contamination.

For Fit NG the separation between neutron and gamma is fixed to the minimum between the two lobes taken from the real curve, whereas for Fit All the minimum is taken from the fitting sum. The area of superposition is shown in Figure 5.37 (a) for Fit NG and (b) for Fit All. For the determination of the area, the position of minimum of the real curve is used for Fit NG while Fit All makes use of the fit curve.

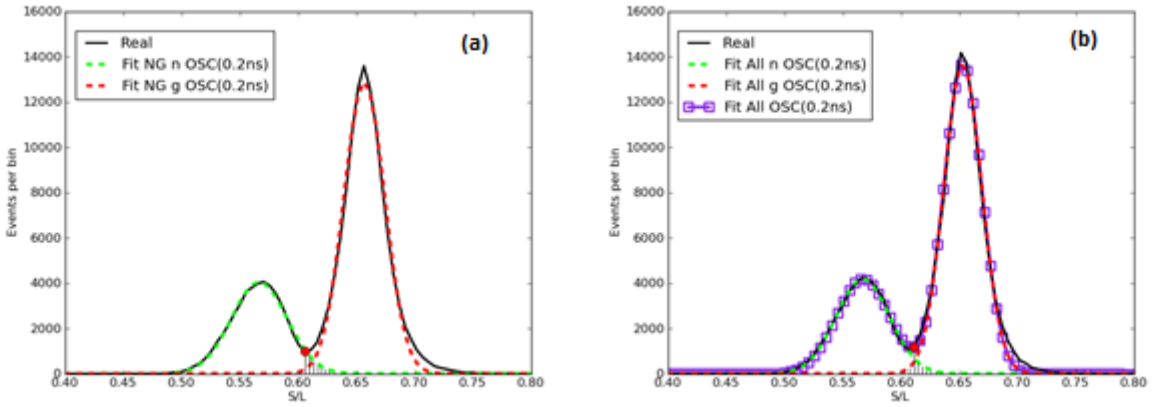

Figure 5.37. Neutron and gamma superposition region for OSC(0.2 ns) dataset for Fit NG (left) and Fit All (right) analysis methods.

The lower is the resolution, the weaker is the separation and the higher is the neutron events amount that breaks through to the gamma left-hand lobe as specified in Table 5.7.

Table 5.7 reports also the FoM_{max} values. Different method of analysis lead to a different FoM_{max} value even if S_{op}/L_{op} are the same (see results for 0.6 ns and 2 ns Fit N and Fit NG). Results are reported in Figure 5.38 for resolutions from 0.2 to 5 ns. The optimal S/L gate combinations are summarized in Table 5.8 with the corresponding FoM_{max} values for the different methods of analysis and time resolutions.

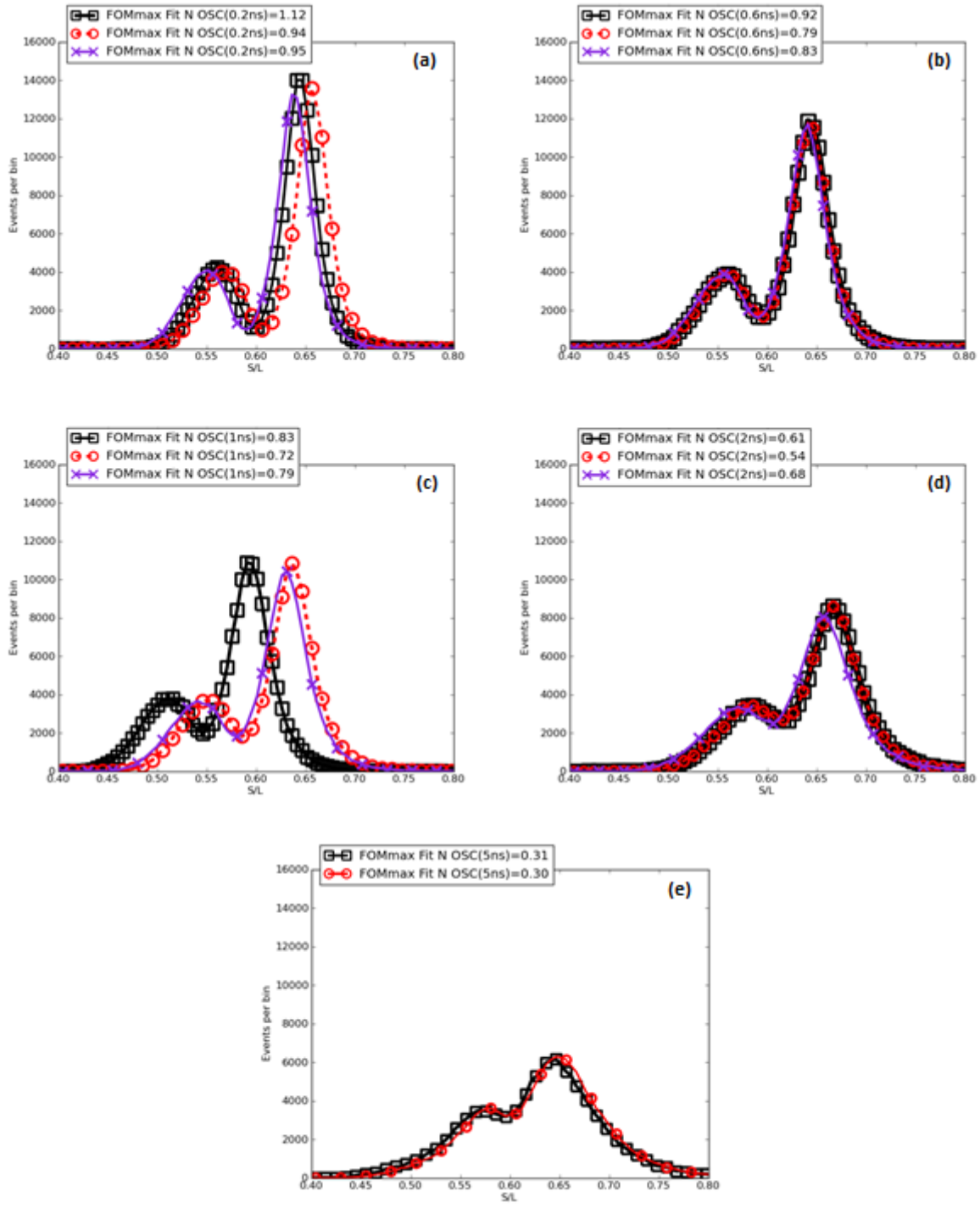

Figure 5.38. S_{op}/L_{op} distribution according to Fit N, Fit NG, and Fit All for OSC (0.2 ns) (a), OSC (0.6 ns) (b), OSC (1 ns) (c), OSC (2 ns) (d) and OSC (5 ns) (e) dataset.

		OSC (Delta pulselength-peak>=64ns)				
		Time resolution				
		0.2ns	0.6ns	1 ns	2 ns	5 ns
	N° waveform dataset	162006	162006	162006	162006	162006
S_{op}/L_{op}	Fit N	8.6/43.6	8.4/48	7/51	8/54	5/65
	Fit NG	9.2/49.6	8.4/48	8/51	8/54	5/55
	Fit All	8.8/51.4	8.4/49.8	8/56	8/62	-
FOM_{max}	Fit N	1.118	0.917	0.825	0.608	0.309
	Fit NG	0.935	0.787	0.717	0.535	0.304
	Fit All	0.945	0.830	0.789	0.676	-

Table 5.8. OSC dataset optimal S_{op}/L_{op} gate combination with their FoM_{max}.

Fit N applied to OSC(0.2 ns) time resolution dataset gives rise to FoM_{max} = 1.118 for S_{op} = 8.6 ns and L_{op} = 43.6 ns, higher than Fit NG where FoM_{max} is equal to 0.935. Fit Gauss2 FoM_{max} results equal to 0.945. For Fit NG and Fit All the optimal gate combination is respectively found for S/L = 9.2 ns/49.6 ns and S/L = 8.8 ns/51.4 ns.

Considering OSC(0.6 ns) dataset, the three method of analysis result in overlapping S/L distribution. Gate optimal combinations are S/L = 8.4 ns/48 ns for Fit N, S/L = 8.4 ns/48 ns for Fit NG and S/L = 8.4 ns/49.8 ns for Fit All.

For OSC(1 ns) dataset (Figure 5.38 (c)), Fit N gives rise to a FoM_{max} = 0.825 (S_{op} = 7 ns, L_{op} = 51 ns), while FoM_{max} = 0.717 (S_{op} = 8 ns, L_{op} = 51 ns). Using Fit All instead FoM_{max} = 0.789 with S_{op} = 8 ns and L_{op} = 56 ns.

It can be noticed that a difference of only one sample in the short gate, leads to a more significant difference than a difference of 5 sample in the long one. In fact extending L gate does not improve the information, which is the opposite of what happens considering 1 more ns of the waveform in the S gate.

As regards OSC(2 ns) time resolution dataset (Figure 5.39 (d)), Fit N gives rise to a FoM_{max} = 0.608 (S_{op} = 8 ns, L_{op} = 54 ns), while FoM_{max} = 0.535 (S_{op} = 8 ns, L_{op} = 54 ns). Using Fit All instead FoM_{max} = 0.676 with S_{op} = 8 ns and L_{op} = 62 ns.

Fit N gives rise to a FoM_{max} = 0.309 (S_{op} = 5 ns, L_{op} = 65 ns), while FoM_{max} = 0.304 (S_{op} = 5 ns, L_{op} = 65 ns) for OSC(5ns) dataset (Figure 5.39 (e)).

FoM_{max} progressively decreases when the oscilloscope data are downsampled. FoM_{max} values and respective percent variation as for 0.2 ns time resolution are summarized in the last rows of Table 5.6.

For Fit N FoM_{max} varies from 1.12 for 0.2ns down to 0.31 for 5 ns time resolution as for KN3 DAQ dataset. For Fit NG from 0.94 to 0.30, and from 0.95 to 0.68 for 2ns for Fit All. Fit All features the smallest variation of FoM_{max} for different time resolutions. As already discussed for the countorplots, this method of analysis, if converging, allows for all the details of S/L distributions to be studied simultaneously. If the oscilloscope sampling rate is reduced to 0.6 ns, FoM_{max} average variation is 18%, while it stays within 29 % and 66% up to 1 and 2 ns respectively. For the same resolution variation are lower using Fit All as for Fit NG and even more compared to Fit N.

This result means that using the full oscilloscope sampling rate capability at 5 GHz, the quality of the n-γ discrimination is on the average more than two fold higher with respect to what obtained at 200 MHz.

The comparison of FoM_{max} obtained for the different time resolution of the oscilloscope data is displayed in Figure 5.39 for Fit NG method of analysis.

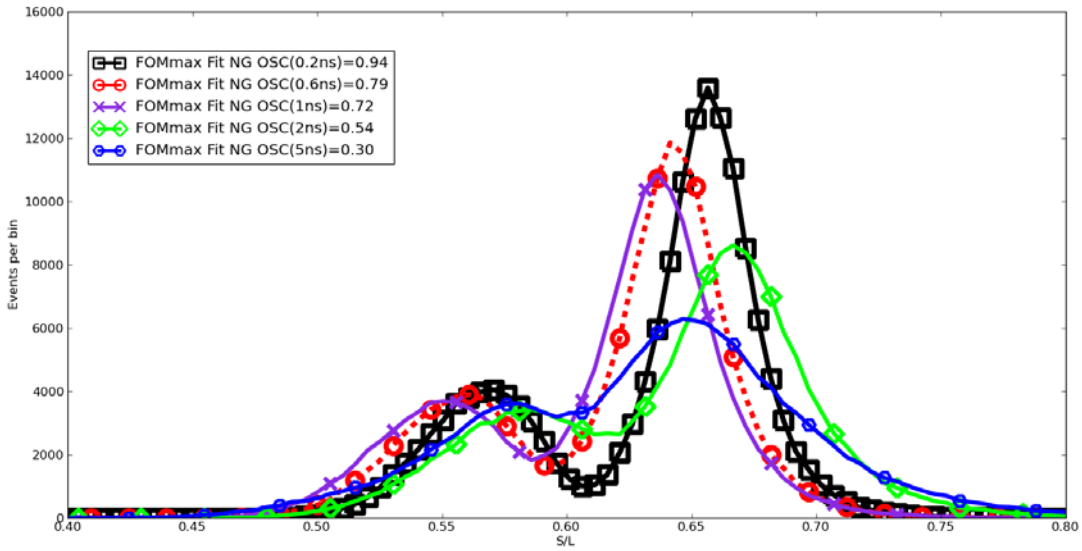

Figure 5.39. Comparison of Fit NG FoM_{max} for different time resolution.

For the same time resolution, different short and long gate combinations results in different shape of the S/L distributions. Figures 5.40 shows the comparison of OSC(0.2 ns) and OSC(2 ns) dataset analyzed, using Fit All method, in terms of S/L distributions obtained considering different S and L gates including the optimal S_{op} and L_{op} (see Figure 5.40).

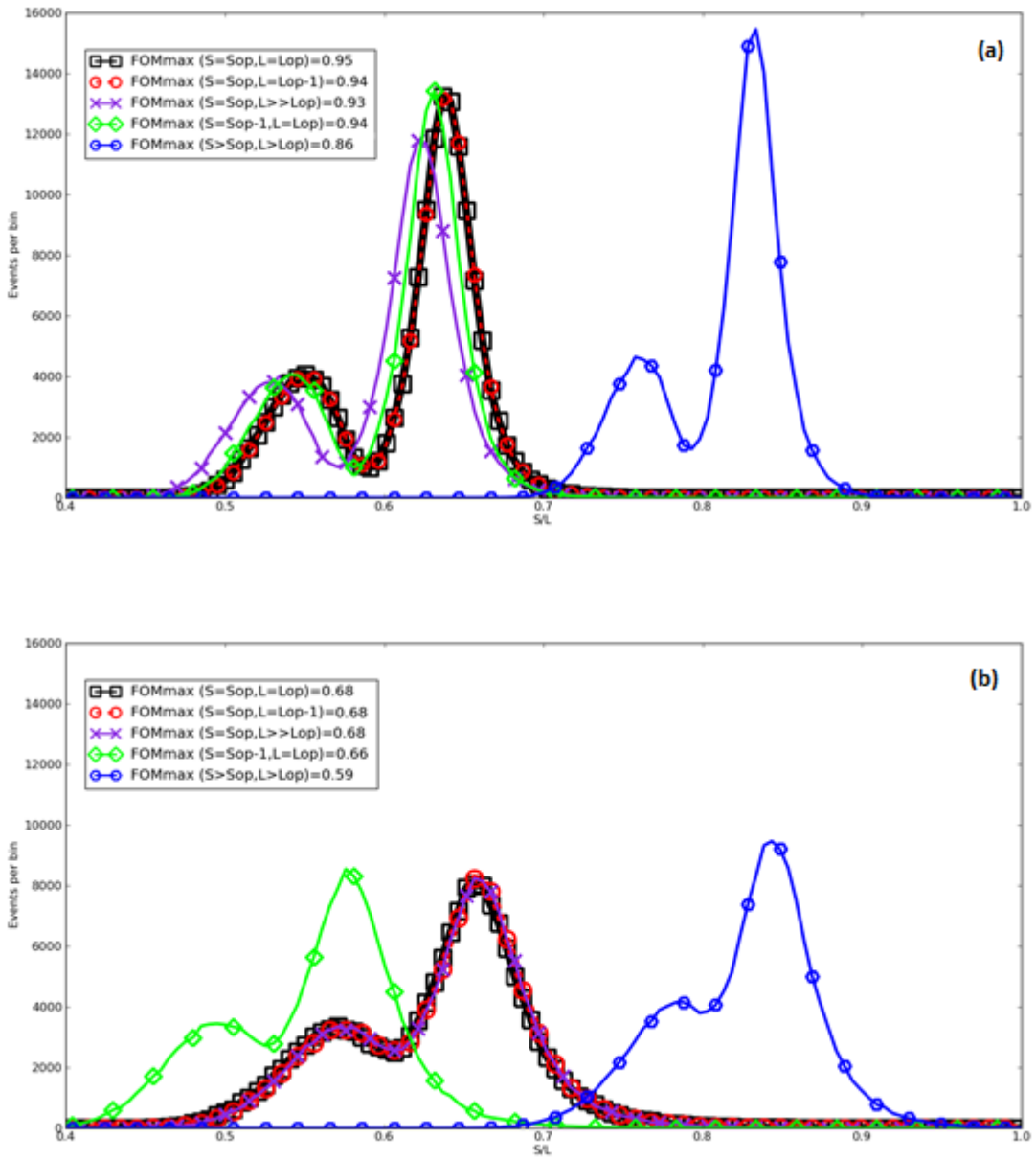

Figure 5.40. Comparison of Fit All S/L distribution for OSC(0.2 ns) (a) and OSC(2 ns) (b) datasets.

For OSC(0.2 ns) dataset, if Fit All method is considered FoM evaluated at L = L_{op}-1decreases of 0.01% compared to the maximum value. Considering L >> L_{op} it is of 1.5% lower and located at the left side of the S/L axis. When S = S_{op}-1 the variation is equal to 0.02%, lower than the one obtained with L = L_{op}-1. S > S_{op} and L > L_{op} variation is the highest compared to the previous cases and equal to 8%.

As regards OSC(2 ns) dataset, Figure 5.40 (b), using L gates different from the optimal value does not result in FoM variations. As just mentioned, extending the long gate alone does not improve the

additional information in terms of n-γ discrimination. Contrarily, FoM obtained using 1 more ns of the waveform in the S gate FoM decreases of 3% and of 13% for $S > S_{op}$ and $L > L_{op}$.

The previous analysis can be applied to OSC(5 ns) time resolution dataset and compared to S_{op}/L_{op} distribution for OSC(0.2 ns) dataset obtained using Fit NG (Figure 5.41).

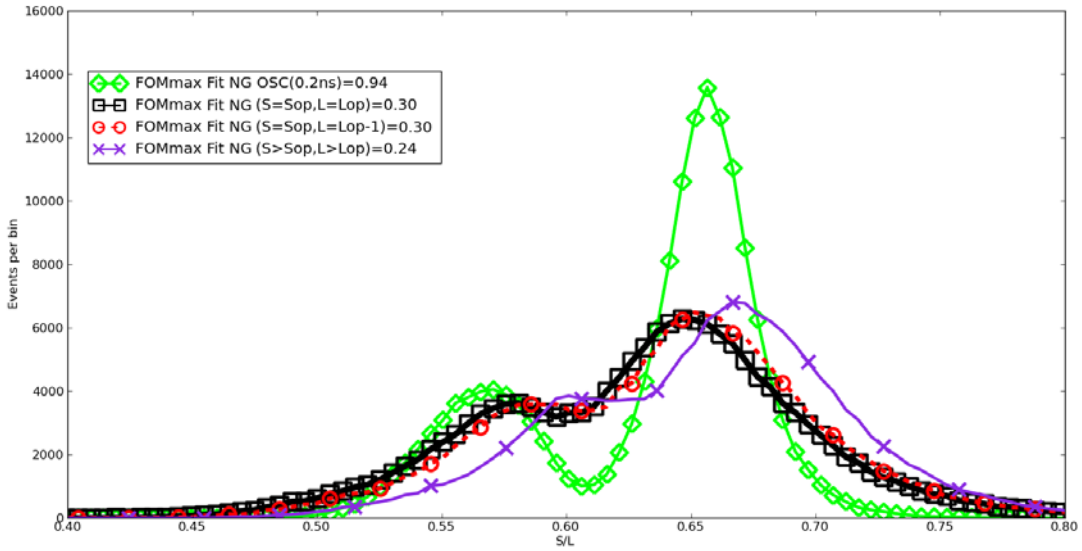

Figure 5.41. Comparison of Fit NG S_{op}/L_{op} distribution for OSC(0.2 ns) with S/L distributions for OSC(5 ns).

The figure displays the redistribution of the neutron and gamma events due to the different time resolution adopted for the study of the same waveforms. Using Fit NG, when $S = S_{op}$ and $L = L_{op}$-1 FoM does not vary from the maximum value of $FoM_{max} = 0.304$. FoM decrease of the 20% when values are far from the optimal choice. OSC(5 ns) dataset analysis lead to the same considerations on the S and L gate choice influence in the n-γ discrimination resulting for the previous OSC time resolutions dataset.

Comparing the 5 ns FoM values considered with the 0.2ns time resolution Fit NG FoM_{max}, variation are respectively equal to 67%, 68% and 74%.

Up to now the time resolution analysis of the oscilloscope data has been pursued always starting from the first sample of the waveform P = 0 sample. This assumption may lead to biased results especially in case of the minimum sampling frequency of 200 MHz. The analysis has been thus repeated using different waveform starting points P. For instance, in case of 1.76 GHz (0.6 ns), only one point out of three is considered in the original waveform. If now the starting point is set to P = 1 sample, a new waveform will be obtained which will be time shifted of 0.6 ns with respect the one

for P = 0 considered previously. For the different time resolution, new waveforms will be obtained which peak might occur at a different amplitude (and sample position) with respect to P = 0.

Figure 5.42 displays the difference between OSC(5 ns) waveforms obtained considering P = 0 sample and P = 20 sample.

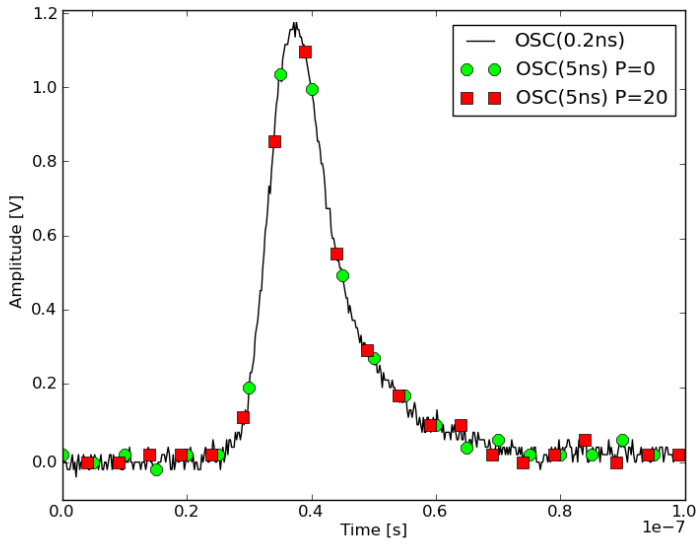

Figure 5.42. OSC(5 ns) obtained from OSC(0.2 ns) but considering P = 0 sample (green dots) and P = 20 sample (red squares).

For the different time resolutions, the OSC dataset can be analyzed with different shifts P. For the different time resolutions different starting point of the waveforms have been considered. In the case of 0.6 ns, for example, one sample each 3 is taken, thus different results can be obtained if P = 0, P = 1 or P = 2. The biggest variations will occur for the lower time resolutions values.

The following waveforms have been considered:

- P = 1 sample for OSC(0.6 ns);
- P = 1 sample and P = 3 samples for OSC(1 ns);
- P = 1 sample, P = 3 samples and P = 5 samples for OSC(2 ns);
- P = [1, 3, 5, 7, 10, 15, 20] for OSC(5 ns).

The results are summarized in the following Table 5.9.

			OSC Dataset filtered (Delta pulselength-peak>=64ns)											
			Time resolution											
			0.6 ns			1 ns			2 ns			5 ns		
	P	Method	S_{op}/L_{op}	FoM_{max}	R	S_{op}/L_{op}	FoM_{max}	R	S_{op}/L_{op}	FoM_{max}	R	S_{op}/L_{op}	FoM_{max}	R
FoM_{max}	1	Fit N	10.2/49.8	0.92	2.47	8/59	0.81	2.38	8/54	0.59	2.23	5/55	0.31	2.05
		Fit NG	9/47.4	0.79	2.48	8/57	0.72	2.45	8/62	0.54	2.39	5/55	0.30	2.05
		Fit All	8.4/49.8	0.84	2.43	8/56	0.79	2.36	8/62	0.68	2.39			
	3	Fit N				9/57	0.82	2.47	8/54	0.62	2.47	5/55	0.29	1.85
		Fit NG				8/53	0.73	2.49	8/54	0.55	2.47	5/55	0.28	1.85
		Fit All				8/56	0.79	2.37	8/58	0.69	2.25			
	5	Fit N							8/54	0.62	2.45	5/50	0.25	1.69
		Fit NG							8/56	0.54	2.52	5/50	0.23	1.69
		Fit All							8/58	0.69	2.40			
	7	Fit N							8/58	0.62	2.41	5/35	0.24	1.26
		Fit NG							8/58	0.54	2.41	5/35	0.22	1.26
		Fit All							8/58	0.69	2.41			
	10	Fit N										5/35	0.24	1.16
		Fit NG										5/35	0.20	1.16
		Fit All												
	15	Fit N										-	-	-
		Fit NG										-	-	-
		Fit All												
	20	Fit N										5/60	0.37	3.04
		Fit NG										5/60	0.37	3.04
		Fit All											-	-

Table 5.9. Summary of the results of the OSC dataset for different time resolutions and starting sample P of the waveforms.

Beside FoM_{max} value, R is calculated in order to verify the validity of the n-γ discrimination.

R value is always in the range expected for 0.6, 1 and 2 ns time resolution, so the FoM maximum values obtained can be compared to the ones obtained for P = 0.

For 5 ns time resolution, P = [3, 5, 7, 10] gives rise to an R value lower than the range expected from the $^{241}Am/^{9}Be$ branching ratio, the script checks whether R values higher than 2 exist and in this case it takes the nearest value to the maximum. For P = 3 the highest FoM value with P higher than 2 is found for OSC (5 ns) for S/L = 5 ns/60 ns and S/L = 5 ns/50 ns, respectively for Fit N and Fit NG. R is now equal to 2.169 and 2.118 and FoM is 0.257 and 0.259 respectively for Fit N and Fit NG. R values calculated for P = [5, 7] are never higher than 2, so even if FoMs are found they are not considered.

Depending on the P value considered, FoM_{max} values could be either higher or lower compared to the P = 0 values. Percent variations are also summarized in Table 5.10.

			OSC Dataset filtered (Delta pulselength-peak>=64ns)							
			Time resolution							
	P	Method	0.6ns		1 ns		2 ns		5 ns	
FoM_{max}	0	Fit N	0.92		0.83		0.61		0.31	
		Fit NG	0.79		0.72		0.54		0.30	
		Fit All	0.83		0.79		0.68		-	
	1	Fit N	0.92	0.2%	0.81	-1.6%	0.59	-2.3%	0.257	-17.0%
		Fit NG	0.79	0.5%	0.72	1.0%	0.54	0.2%	0.259	-14.8%
		Fit All	0.84	0.7%	0.79	0.6%	0.68	0.6%	-	-
	3	Fit N			0.82	-0.1%	0.62	2.1%	0.287	-7.1%
		Fit NG			0.73	1.3%	0.55	2.2%	0.280	-7.9%
		Fit All			0.79	0.4%	0.69	1.5%	-	-
	5	Fit N					0.62	2.1%	0.247	-20.1%
		Fit NG					0.54	1.5%	0.23	-24.3%
		Fit All					0.69	1.3%	-	-
	7	Fit N					0.62	2.6%	0.24	-21.7%
		Fit NG					0.54	1.5%	0.22	-28.0%
		Fit All					0.69	1.5%	-	-
	10	Fit N							0.24	-23.0%
		Fit NG							0.20	-35.5%
		Fit All							-	
	15	Fit N							-	-
		Fit NG							-	-
		Fit All							-	-
	20	Fit N							0.37	18.1%
		Fit NG							0.37	20.7%
		Fit All							-	-

Table 5.10. Different P analysis results compared with P = 0.

For OSC(0.6 ns) time resolution, FoM_{max} for P = 1 is slightly lower with respect to P = 0 for all the methods of analysis.

For OSC(1 ns), P = 1and P = 2 give rise to lower FoM_{max} values for Fit N, Fit NG and Fit All instead lead to higher values.

FoM_{max} values calculated for OSC(2 ns) time resolution, with the exception for FoM_{max} calculated using Fit N for P = 1, considering the different P for the all the methods of analysis.

OSC(5 ns) FoM_{max} values are always lower if compared with the ones obtained for P = 0, with the exception of P = 20, which gives rise to values about 20% higher.

The analysis conducted so far refers to 162006 waveforms, for which difference between length and peak position gives rise to a delta larger than L_{max} = 64 ns. If the whole OSC dataset of 202000 waveforms is considered, zeros will be added to calculate $L > L_{max}$ = 64 ns, if the waveform presents a delta shorter than $L_{max.}$

Results of this analysis are reported in Table 5.11 for 1, 2, 5 ns time resolution and compared with the ones obtained in the previous analysis.

		OSC Dataset filtered (Delta pulselength-peak>=64ns)			OSC Whole dataset		
		Time resolution			Time resolution		
		1 ns	2 ns	5 ns	1 ns	2 ns	5 ns
	N° waveform dataset	162006	162006	162006	202000	202000	202000
N° waveform in S/L distribution	Fit N	162002	162001	161982	201995	201994	201975
	Fit NG	162003	162001	161967	201996	201996	201963
	Fit All	162002	162000	-	201996	201994	-
S_{op}/L_{op}	Fit N	7/51	8/54	5/65	9/55	8/50	5/60
	Fit NG	8/51	8/54	5/55	8/62	8/62	5/55
	Fit All	8/56	8/62	-	9/58	8/58	-
FOM_{max}	Fit N	0.83	0.61	0.31	0.70	0.52	0.38
	Fit NG	0.72	0.54	0.30	0.63	0.46	0.36
	Fit All	0.79	0.68	-	0.68	0.58	-
FOM_{max} variation	Fit N	-	-	-	-15%	-15%	23%
	Fit NG	-	-	-	-13%	-15%	17%
	Fit All	-	-	-	-14%	-14%	-
R (minimun real distribution)	Fit N	2.29	2.38	2.62	2.41	2.47	2.14
	Fit NG	2.42	2.25	2.69	2.45	2.47	2.49
	Fit All	2.30	2.25	-	2.36	2.22	-

Table 5.11. Comparison of the results obtained considering the full OSC dataset of 202000 waveforms with respect of the ones for 162006 with $L \geq L_{max}$.

Optimal parameters are different if the whole database is considered.

For OSC(1 ns) time resolution the optimal S-L gates are higher if compared with the filtered dataset, for all the methods of analysis.

For OSC(2 ns) time resolution instead, the S_{op} is the same with respect of the filtered dataset while L_{op} is lower for Fit N and Fit All and higher for Fit NG.

The optimal gates differ for OSC (5 ns) only for L_{op} calculated with Fit N, which is lower compared to the filtered dataset one.

Comparing the results in terms of FoM_{max}, lower values are obtained for OSC(1 ns) and OSC(2 ns) with the all methods of analysis, while for OSC(5 ns) time resolution Fit N and Fit NG methods give rise to higher values with respect of the filtered dataset.

Figure 5.43 shows results for the filtered and the whole OSC datasets, for the different time resolutions considered, for Fit NG method.

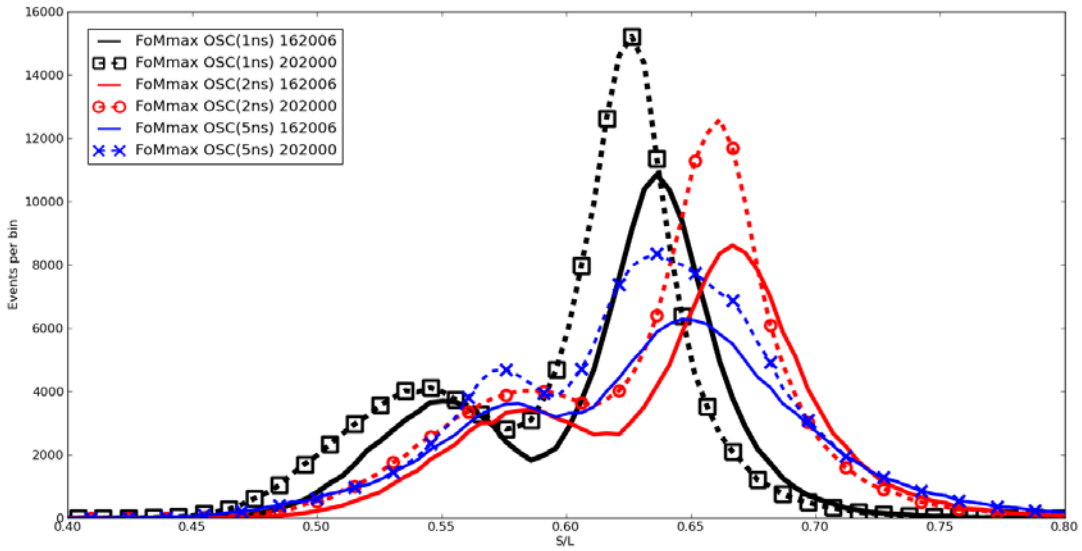

Figure 5.43. Comparison of the filtered and the whole OSC datasets in terms of the optimal gate S/L distributions.

FoM_{max} values are on average 14% lower than the ones obtained for the filtered dataset. They are about 20% higher for 5ns. This can be interpreted as the results of processing waveforms with duration lower than $L_{.max}$. In this case the script adds zeros when the end of the tail is overcome. Since percent variations are low as for the dataset filtered, evaluating FoM values through

integrating the tail of the pulse moving the long gate each sample, does not give significant contribute in term of PSD since pulse values in the tail is comparable with the noise.

R is always in the range expected so FoM_{max} values can be considered and compared.

DAQ data

The data recorded with the KN3 digital acquisition system (200 Msamples/s sampling rate and 14 bit resolution) have been analyzed to determine the optimal gate combination S_{op} and L_{op} to maximize the n-γ discrimination and to compare this results with the ones obtained from the OSC dataset at different time resolution. Unlike the OSC dataset, the DAQ waveforms feature different lengths, as shown in Figure 5.14. Difference between the length and the peak position of the waveforms are always higher than 64 ns. The waveforms were recorded using an hardware threshold of 80 mV. Figure 5.44 shows example of DAQ waveforms.

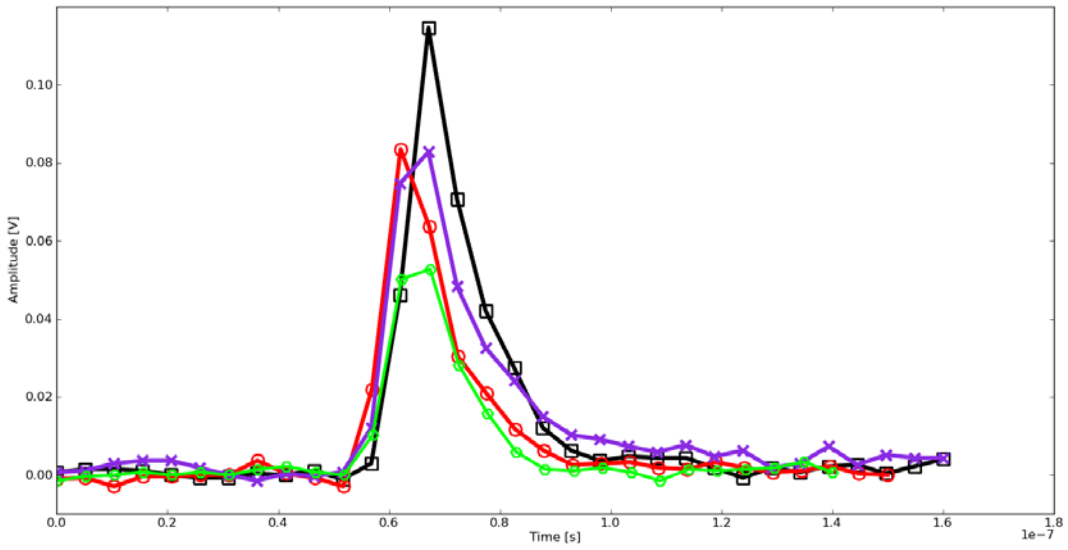

Table 5.44. Examples of DAQ waveforms, which feature different lengths and peak positions.

For the DAQ dataset analysis and comparison with OSC results, a software threshold of 110 mV have been used to process the DAQ waveforms such that only 165118 waveforms were selected. This to have a comparable statistics between OSC and DAQ results.

The DAQ dataset have been studied with the same Python script [11] using Fit N, Fit NG and Fit All analysis method for the FoM calculation.

The time resolution is 5 ns. As mentioned in the first section, 200 bins have been selected for the S/L distributions to calculate the FoM values. The contour plots are displayed in Figure 5.45.

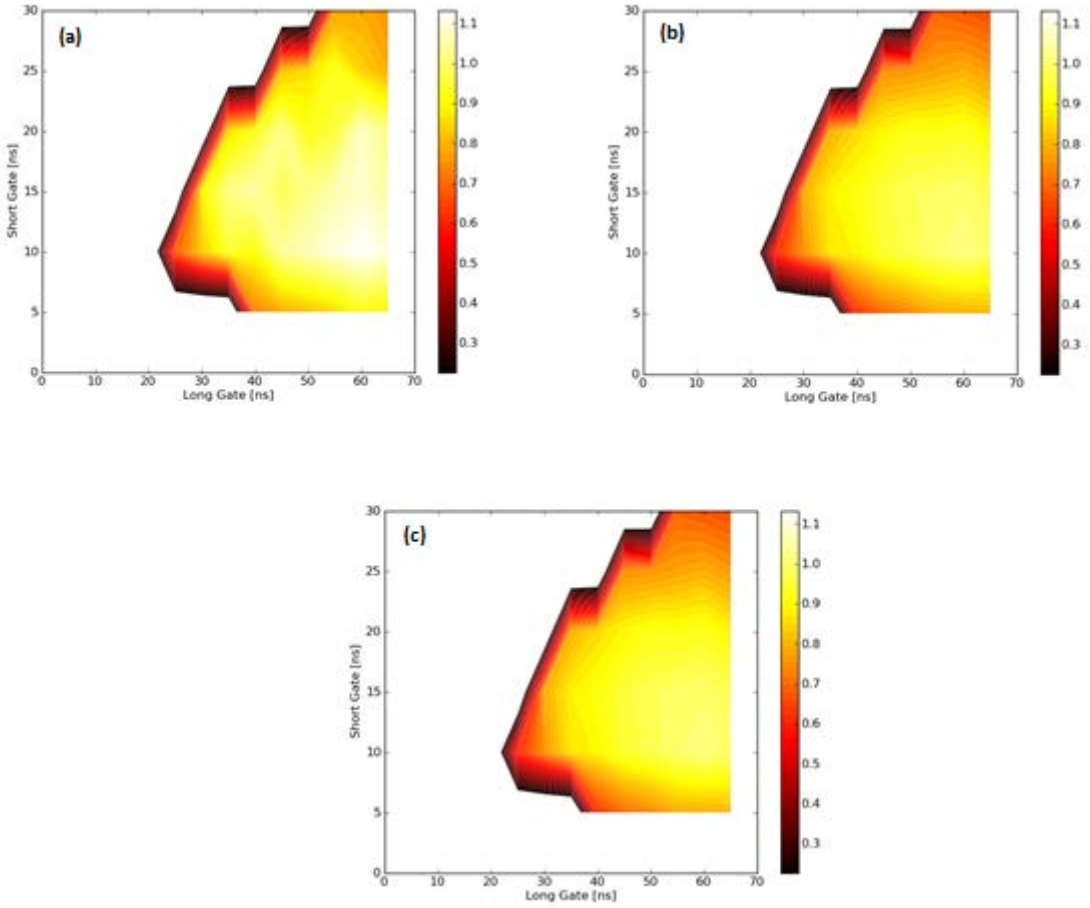

Figure 5.45. FoM Contour plots of the DAQ dataset analyzed with a software threshold of 110 mV and with Fit N (a), Fit NG (b) and Fit All (c) methods.

Different regions can be recognized in Figure 5.45 (a). The white region outside the contour plot border features no events. This results in the sharp boarder of the contour plot with steep gradients. A region with FoM > 1 can be recognized for gate S = [5, 20] ns and for L = [35, 65] ns which is a quite wide range. Inside this region, the area with FoM > 1.1 is defined by S=[5, 15] ns and L = [50, 60] ns which give rise to well separate lobes. Using Fit NG method (Figure 5.45 (b)) contour plot looks more homogeneous than the previous one since in this method $FWHM_{\gamma}$ derives from the output of the fit of both neutron and gamma lobes separately. FoM values are also on average lower than for Fit N analysis. As for Fit N, a region with FoM > 0.9 can be recognized for gate S = [5, 21] ns and for L = [5, 65] ns. The region of FoM > 1.1 corresponds to S = [10, 15] ns and to L = [50, 60] ns. FoM rapidly decreases to values below 0.3 considering either one sample of the

waveform immediately after the peak or increasing the portion of the trailing edge after 15 ns (three sample after the waveform peak). These two region do not improve much the n-γ discrimination.

In Fit All the lobes are well separated in a smaller region with respect to Fit NG (Figure 5.45 (c)). The optimal S_{op}/L_{op} distribution of Fit All is displayed in Figure 5.46 (a) together with the sum of Fit NG (i.e. Fit NG Sum) for S_{op} = 10 ns and L_{op} = 60 ns.

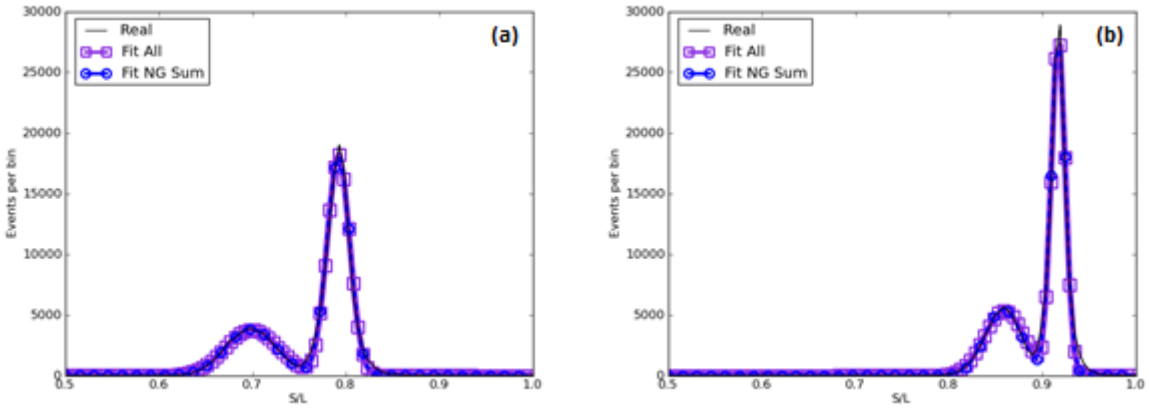

Figure 5.46. Comparison of the S_{op}/L_{op} distributions (a) for Fit All and Fit NG Sum (S_{op} = 10 ns and L_{op} = 60 ns) and for S = 20 ns and L = 50 ns in (b).

In Figure 5.46 (b) the comparison is made for S = 20 ns and L = 50ns which highlight the lower n-γ separation using Fit All method.

Differently from DAQ, Fit All never converges for OSC(5 ns) dataset and only 6 S/L gate combinations are found using Fit N and Fit NG (see Figure 5.34). In Figure 5.47 a comparison of the S/L distributions for DAQ and OSC(5 ns) considering S = 10 ns and L = 60 ns (i.e., the optimal gate combination for DAQ dataset) is reported. For DAQ S/L distribution Fit All method is represented.

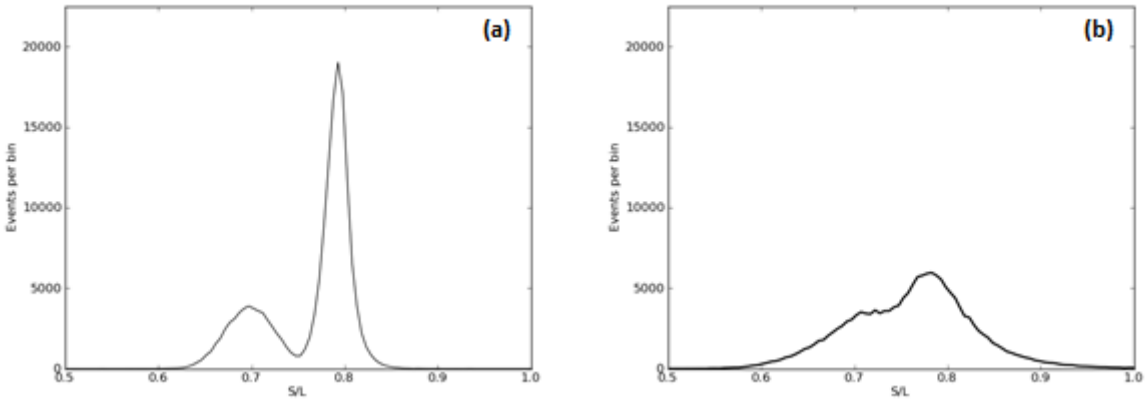

Figure 5.47. Comparison of DAQ and OSC(5 ns) datasets S/L distributions for S = 10 ns and L = 60 ns.

For OSC(5 ns) dataset S = 10 ns and L = 60 ns gate does not give rise to separate lobe, the minimum on the real curve is not found and method of analysis cannot be applied.

Table 5.12 summarizes the results of the analysis with the three methods for the DAQ dataset.

	DAQ (110 mV) N° waveform dataset 165118	
S_{op}/L_{op}	Fit N	10/60
	Fit NG	10/60
	Fit All	10/60
FOM_{max}	Fit N	1.13
	Fit NG	1.02
	Fit All	0.99
R (minimun real distribution)	Fit N	2.32
	Fit NG	2.32
	Fit All	2.32
R (minimun fit tot)	Fit NG	2.22
	Fit All	2.17

Table 5.12. Comparison of the optimal gate combinations S_{op} and L_{op} and the corresponding FoM_{max} and γ/n ratio obtained with Fit N, Fit NG and Fit All methods for the analysis of the DAQ dataset.

For the same threshold the same S/L combination is found as optimal for the three method used which comparison is reported in Figure 5.48 with other two distributions (S = Sop , L = Lop-1) and (S > Sop, L > Lop).

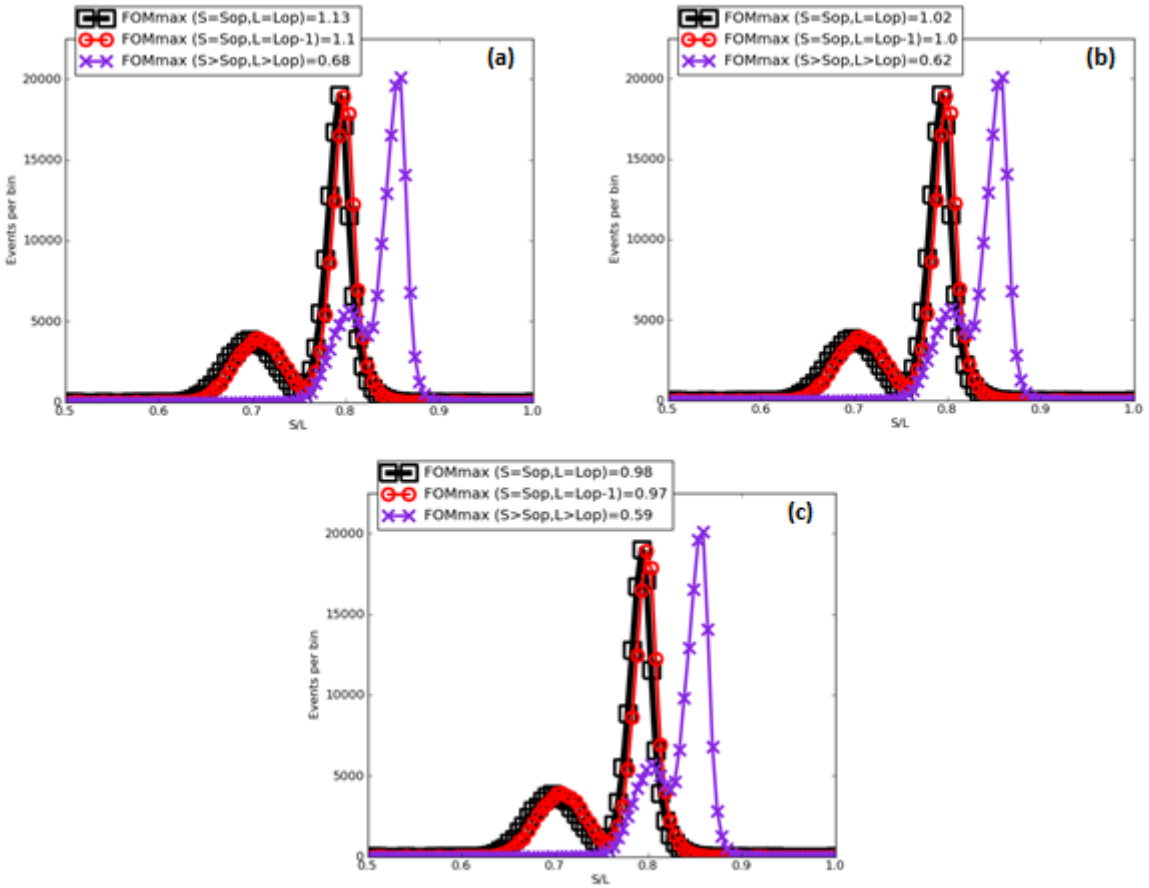

Figure 5.48. Comparison of the S/L distributions obtained using Fit N (a), Fit NG (b) and Fit All (c) methods of analysis. The S_{op}/L_{op} distribution is compared with other two ($S=S_{op}$, $L=L_{op}-1$ and $S>S_{op}$, $L>L_{op}$).

For Fit N method (Figure 5.48 (a)) when L is set one sample lower than the optimal value the FoM is lower of the 2.6%, and decrease of 40% when S and L optimal gate are far from the optimal values. As mentioned in the OSC analysis, this latter distribution is located in the right side of the S/L axis since even if gates are both higher than the optimal choice, the short gate integral increasing weight more than the long gate one.

For Fit NG method (Figure 5.48 (b)) when L is set one sample lower than the optimal value the FoM is lower of the 2.3%, and decrease of 40% when S and L optimal gate are far from the optimal values. Variations are the same of Fit N method.

For Fit All method (Figure 5.48 (c)) when L is set one sample lower than the optimal value the FoM is lower of the 1.7%, and decrease of 40% when S and L optimal gate are far from the optimal values. Variations are comparable with the ones obtained for the previous methods.

Differences in FoM values can be explained from different parameters used in the calculation for the three methods of analysis of DAQ dataset.

	Fit N	Fit NG	Fit All
$S_{n-\gamma}$	0.0943	0.0935	0.0928
$FWHM_n$	0.0630	0.0631	0.0661
$FWHM_\gamma$	0.0202	0.0285	0.0281
FoM	1.133	1.021	0.985

Table 5.13. FoM parameters for Fit N, Fit NG and Fit All.

The ratio R of gamma and neutron events is within 2.1 and 2.8. Since the same methods of analysis has been as for OSC data, the R space of phase has been analyzed considering the whole short and long gate combination. The contour plot of figure 5.49 reports the results.

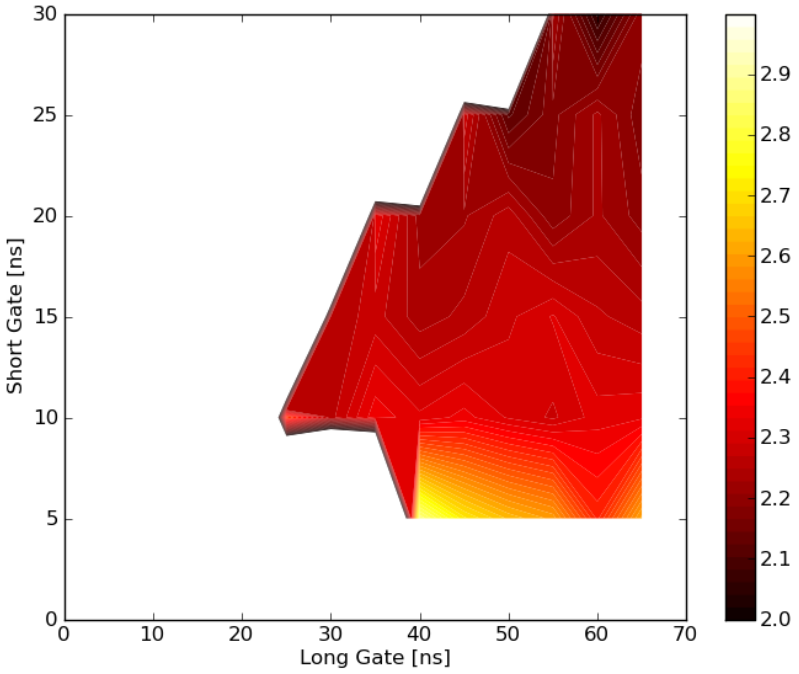

Figure 5.49. R contour plot for the DAQ dataset with 110 mV threshold.

R varies up to 2.8 and it is always in the range expected from the branching ratio. The scatter plots FoM vs R are shown in Figure 5.50 For the three methods of analysis.

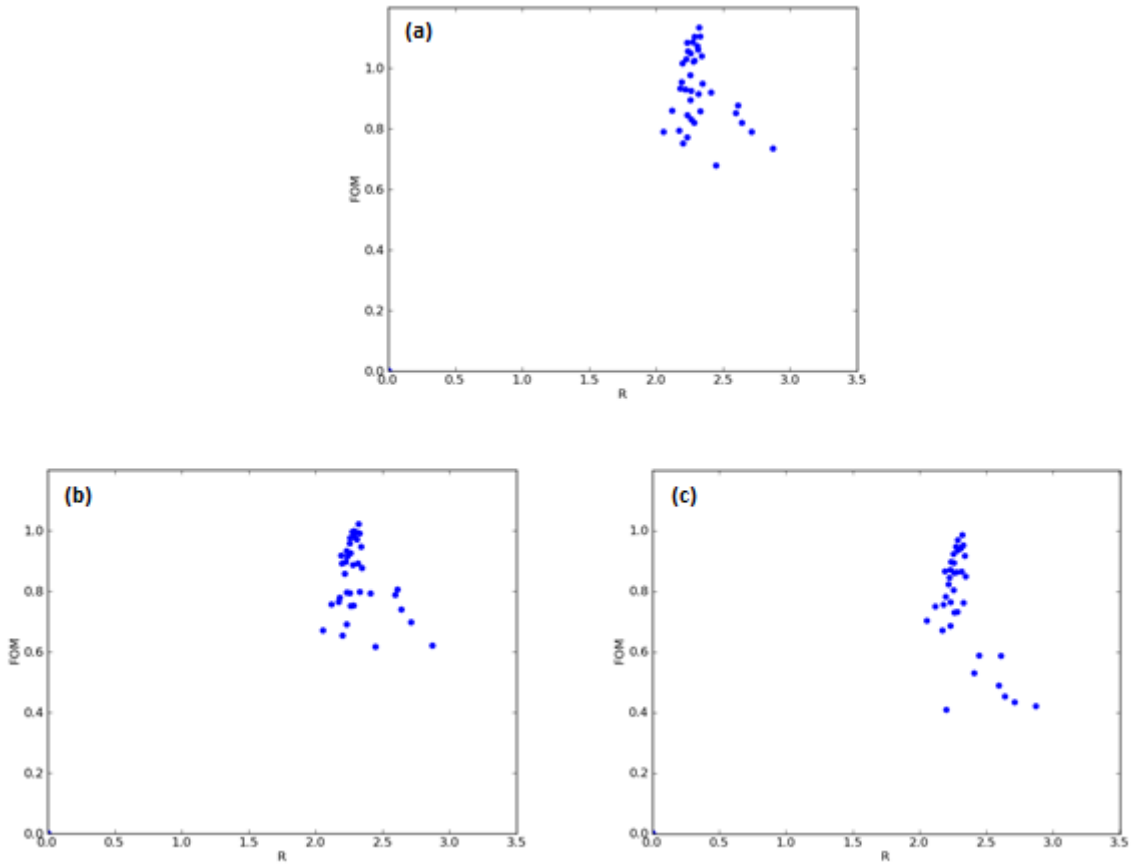

Figure 5.50. FoM vs R scatter plots for the DAQ dataset for Fit N (a), Fit NG (b), and Fit All (c).

Here the FoM_{max} corresponds to R = 2.3 while R = 2.8 results from S/L distributions with neutron and gamma lobes not well separated (FoM ≤ 0.8). For OSC dataset (Table 5.6) R is about 2.5 for all time resolutions up to 2 ns. For OSC(5 ns) it results 2.1 for Fit N and 2.5 for Fit NG. These results for OSC are similar to the ones obtained for DAQ dataset such that the $^{241}Am/^{9}Be$ γ/n ratio of 2-3 corresponds to FoM_{max} calculated from the S_{op}/L_{op} distribution.

Instead of considering the minimum of the S/L distributions, R has been evaluated also considering the minimum of the total fit, respectively for Fit NG and Fit All. Since neutron and gamma lobes are well separated in the optimal S/L gate combination distribution, the superposition of events is low, as shown in picture 5.51.

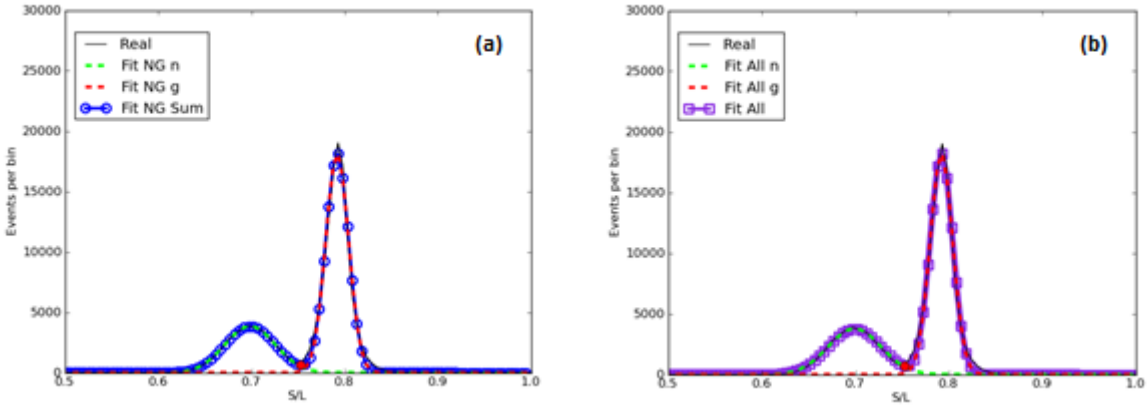

Figure 5.51. Comparison of Fit NG Sum (a) and Fit All (b) analysis for S_{op} = 10 ns and L_{op}= 60 ns.

For each S/L distribution it is possible to determine the level of the contamination, i.e. neutron events into the gamma lobe (n_γ) and gamma events into the neutron lobe (γ_n).

Using the S_{op}/L_{op} distribution n_γ and γ_n have been determined and the results reported in Table 5.14. Applying the same analysis as for OSC dataset, the separation between neutron and gamma is fixed to the minimum of the S_{op}/L_{op} distribution on the real curve for Fit NG, whereas in Fit All the minimum is taken on the fit.

	DAQ (110 mV) N° waveform dataset 165118	
n_γ [events]	Fit NG	2203
	Fit All	1931
γ_n [events]	Fit NG	29
	Fit All	107
S_{op}/L_{op}	Fit N	10/60
	Fit NG	10/60
	Fit All	10/60
N° waveform in S/L distribution	Fit N	165118
	Fit NG	165118
	Fit All	165118

Table 5.14. n_γ and γ_n events in the S_{op}/L_{op} distribution for DAQ dataset.

As displayed in Figure 5.51 n_γ is consistently higher than γ_n with n_γ similar for Fit NG and Fit All methods. The S_{op}/L_{op} distribution results for S = 10 ns and L = 60 ns.

Discussions

The results presented are summarized in Table 5.15.

The OSC and The DAQ results show that:

- The third method of analysis of the S/L distributions (Fit All) gives rise to the minimum variations in the FoM phase space. This is due to the convergence of the fitting function, sum of two Gaussians, which is a better and more robust method of analysis;
- The higher time resolution allows for a shorter L gate such that shorter pulses can be recorded increasing the acquisition rate. The comparison of OSC(0.2 ns)-OSC(5 ns) and DAQ datasets shows that higher sampling rate allows optimal PSD discrimination for shorter long gates L_{op} such that the pulse length of the recorded signals can be reduced allowing for higher acquisition rates. This will be important for the design of digital data acquisition systems for neutron diagnostics implemented in ITER in view of the high neutron emission rates;
- FoM_{max} progressively decreases when the oscilloscope data are down sampled. Using the full oscilloscope sampling rate capability at 5 Gsamples/s, the quality of the n-γ discrimination is on the average more than twofold larger with respect to what obtained at 200 MHz;
- OSC(5 ns) dataset, comparable to DAQ dataset, provides poor results in terms of n-γ discrimination. DAQ dataset gives rise to FoM_{max} threefold larger with respect to what obtained for OSC(5 ns) and comparable instead with OSC(0.2 ns) FoM_{max} values. This fact can be probably due to the different measurement conditions (cabling and amplification) and bit resolution;
- For the optimal S_{op}/L_{op} gate distributions for both OSC and DAQ data, R consistent with the range expected from the $^{241}Am/^{9}Be$ branching ratio.

		OSC					DAQ (110mV)
		0.2ns	0.6ns	1 ns	2 ns	5 ns	
	N° waveform dataset	162006	162006	162006	162006	162006	165118
N° waveform in S/L distribution	Fit N	162003	162003	162002	162001	161982	165118
	Fit NG	162002	162003	162003	162001	161967	165118
	Fit All	162002	162002	162002	162000	-	165118
S_{op}/L_{op}	Fit N	8.6/43.6	8.4/48	7/51	8/54	5/65	10/60
	Fit NG	9.2/49.6	8.4/48	8/51	8/54	5/55	10/60
	Fit All	8.8/51.4	8.4/49.8	8/56	8/62	-	10/60
FOM_{max}	Fit N	1.12	0.92	0.83	0.61	0.31	1.13
	Fit NG	0.94	0.79	0.72	0.54	0.30	1.02
	Fit All	0.95	0.83	0.79	0.68	-	0.99
R (minimun real distribution)	Fit N	2.54	2.53	2.41	2.47	2.14	2.32
	Fit NG	2.53	2.53	2.45	2.47	2.49	2.32
	Fit All	2.48	2.44	2.36	2.22	-	2.32
R (minimun fit sum)	Fit NG	2.47	2.66	2.55	-	-	2.22
	Fit All	2.45	2.36	2.49	2.48	-	2.17
n_γ [events]	Fit NG	2236	4854	6932	15329	34172	2203
	Fit All	2146	3101	5234	7566	-	1930
γ_n [events]	Fit NG	572	1303	1651	4073	14903	29
	Fit All	473	999	984	2302	-	107

Table 5.15. Comparison of the S_{op}/L_{op} gate combination and the corresponding FoM_{max} and n/γ ratio for OSC and DAQ datasets.

For the S_{op}/L_{op} distribution study, it is better to consider waveforms with $L > L_{max}$ such that no deterioration is brought about in the S/L distribution evaluation [13]. OSC(5 ns) and DAQ, even if the statistic is comparable present different results, explainable in differences in the acquisition settings. The OSC data were recorded with amplification x8 and 230 mV threshold while DAQ with gain x4 and 80 mV threshold. The pulse height distributions, i.e. area of the waveforms, are shown in Figure 5.52 The OSC and DAQ bit resolution plays also an important role. The integral distribution is plotted for the whole set of oscilloscope time resolutions and the DAQ dataset.

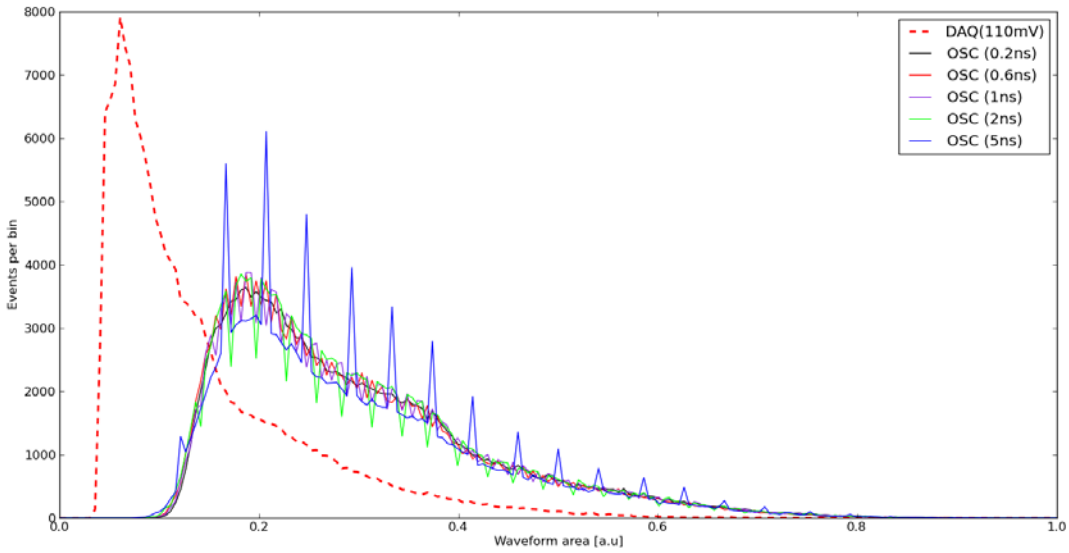

Figure 5.52 Comparison of the pulse height spectra obtained for DAQ and OSC datasets.

OSC and DAQ dataset presents integral peaked on different values. For OSC dataset, lowering the time resolutions, results in pulse height spectra featuring spikes.

The S_{op}/L_{op} distributions for OSC(5 ns) and for DAQ(10 ns/60 ns) are shown in Figure 5.53. The distributions are not comparable.

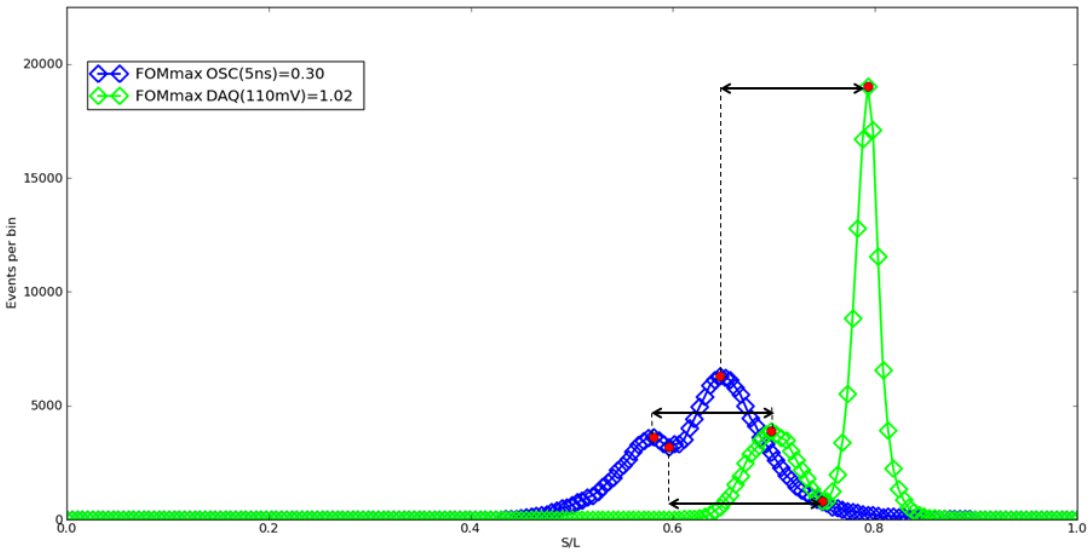

Figure 5.53 S_{op}/L_{op} distributions for OSC(5 ns)and DAQ datasets using Fit NG method.

The comparison of the normalized average neutron and gamma waveforms for OSC(5 ns) and DAQ is displayed in Figure 5.54.

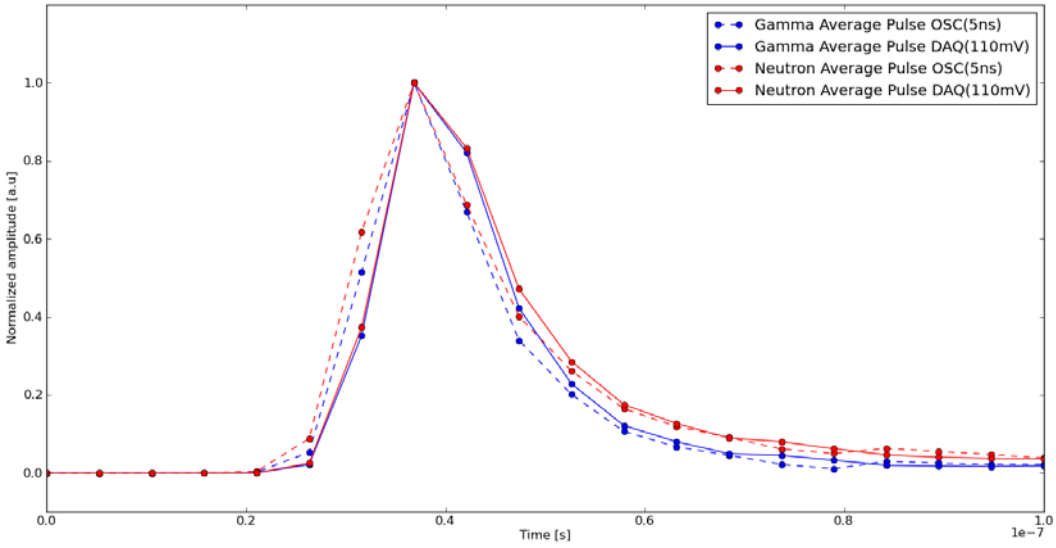

Figure 5.54 Comparison of the normalized neutron and gamma waveforms for OSC(5ns) and DAQ datasets.

The figure shows the different shapes, due to different cabling and amplification. OSC(5 ns) shows a steeper rise and sharp peak. Though lower amplification, DAQ shows a hump on the waveform 5 ns after peak. Though lower amplification DAQ shows a hum on the waveform 5 ns after peak. This is related to the different bit resolution which seems having bigger effects on OSC(5 ns) dataset.

Furthermore since a sensible difference on the rising edge is evident on the OSC(5 ns) average neutron and gamma waveforms, high sampling rate would also allow for the exploitation of the rising edge of the waveforms for n-γ discrimination. This would result in a much faster digital data acquisition system since the waveforms could be recorded up to few samples after the peak.

For this reason OSC(0.2 ns) neutron and gamma average pulses have been considered and displayed in Figure 5.55. A slight difference in the rising edge still exists.

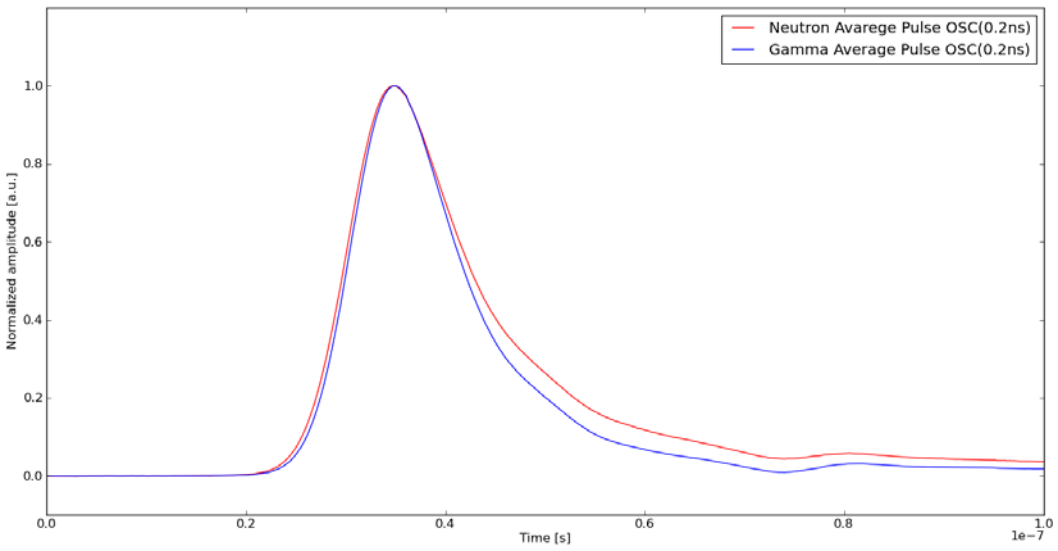

Figure 5.55 Normalized neutron and gamma waveforms for OSC(0.2 ns) and DAQ datasets.

The hump in DAQ waveforms results in $S_{(DAQ)} > S(_{OSC(5\ ns)})$ such that the S/L distribution for DAQ is shifted to higher values (Figure 5.53).

Values obtained are reported in Table 5.16 together with the percent variation of the peak positions.

	DAQ(110 mV)	OSC(5 ns)	Variation
Gamma peak position [ns/ns]	0.793	0.656	21%
Neutron peak position [ns/ns]	0.697	0.571	22%
Gamma S_{op} integral [a.u. · s]	2.244	1.669	34%
Gamma L_{op} integral [a.u.·s]	2.874	2.539	13%
Neutron S_{op} integral [a.u.·s]	2.305	1.688	37%
Neutron L_{op} integral [a.u.·s]	3.284	3.001	9%
Gamma S_{op}/L_{op} integral [a.u.·s]	0.781	0.657	19%
Neutron S_{op}/L_{op} integral [a.u.·s]	0.702	0.562	25%

Table 5.16. DAQ and OSC mean gamma and neutron pulses distribution peak positions and S_{op}/L_{op} variations.

Neutron and gamma peak position variations are equal to 20% and 23% respectively. S_{op} and L_{op} variations between DAQ and OSC evaluated for the average gamma pulse is 34% and 13% respectively, giving rise to a S_{op}/L_{op} = 19 %. The same variation applied on neutron mean pulse gives S_{op}/L_{op} = 25%. FoM_{max} are different for OSC(5 ns) and DAQ because of the "hump" at the first point after peak which results in the S/L distributions shift.

Though the cabling and amplification, the analysis conducted thus demonstrate that increasing the time resolution to 5GHz compensate the bit resolution difference. In Table 5.15 FoM_{max} for OSC(0.2 ns) and DAQ are similar. The use of 5GHz-8bit oscilloscope results in a more efficient acquisition (shorter pulses) if compared to the standard 200 Msamples/s-12 bit. An higher time resolution potentially allows for a more accurate and fast data acquisition simultaneously which is useful in view of ITER nuclear fusion experiments when higher neutron rate emission is foreseen.

Conclusions

The study presented illustrates the comparison of the analysis of signals neutron and γ radiation from the $^{241}Am/^{9}Be$ neutron source induces in KN3 channel 4. The signals were recorded as waveforms using two different digital acquisition systems. The first digital acquisition system is the oscilloscope TekTronix TDS3034B (OSC) operated at 5 Gsamples/s sampling rate and 8 bit resolution and featuring a slow acquisition rate of 3 waveforms/s. The second digital acquisition system (DAQ) is capable of 200Msamples/s sampling rate and 14 bit resolution and high acquisition rate.
A preliminary study has been conducted to assess the analysis methods for Pulse Shape Discrimination (PSD) and the effects of sampling rate/bit resolution on the results.

The PSD analysis has been carried out by using the charge comparison method as implemented in the DAQ system. The Figure of Merit (FoM) has been exploited as a parameter to quantify the efficiency of n-γ discrimination of the PSD method. Though cabling and amplification, this study has investigated three methods for the analysis of the S/L distributions for the FoM calculation:

a. Gaussian fit of the neutron lobe and real γ lobe;

b. Gaussian fits of the neutron and γ lobes separately;

c. Double Gaussian fit of the S/L distribution.

Since the $^{241}Am/^{9}Be$ neutron and γ branching ratio is known, the optimal gate combination S_{op}-L_{op}, which give rise to the FoM maximum value, was tested considering the ratio R of the total gamma and neutron events of the lobes of the S_{op}/L_{op} gate distribution. The test proved consistent with the $^{241}Am/^{9}Be$ branching ratio of R = (gamma events / neutron events)$|_{Sop\text{-}Lop}$ about 2-3.

In order to investigate the effect of the time resolution on the n-γ discrimination, the OSC data have been down sampled up to the time resolution of the KN3 DAQ (5 ns).

Results in terms of FoM phase space for all S-L gate combinations for OSC and KN3 DAQ data have been reported according to the different methods of analysis. The optimal S-L gate settings have been determined for both datasets.

Analyzing the results for the whole set of OSC time resolutions, the following results can be highlighted:

- The third method of analysis of the S/L distributions (Fit All) gives rise to the minimum variations in the FoM phase space. This is due to the convergence of the fitting function, sum of two Gaussians and subsequently more robust and thus, the best method of analysis;
- FoM_{max} progressively decreases when the oscilloscope data are down sampled. Using the full oscilloscope sampling rate capability at 5 Gsamples/s, the quality of the n-γ discrimination is on the average more than twofold larger with respect to what obtained at 200 MHz;
- OSC(5 ns) dataset, comparable to DAQ dataset, provides poor results in terms of n-γ discrimination. DAQ dataset gives rise to FoM_{max} threefold larger with respect to what obtained for OSC(5 ns) and comparable instead with OSC(0.2 ns) FoM_{max} values. This fact can be related to the different measurement conditions (cabling and amplification) and bit resolution;
- For the optimal S_{op}/L_{op} gate distributions for both OSC and DAQ data, R is always in the range 2-3 as expected from the $^{241}Am/^{9}Be$ branching ratio;
- The comparison of OSC(0.2 ns)-OSC(5 ns) and DAQ datasets show that higher sampling rate allows optimal PSD discrimination for shorter long gates L_{op} such that the pulse length of the recorded signals can be reduced allowing for higher acquisition rates. This will be important for the design of digital data acquisition systems for neutron diagnostics implemented in ITER in view of the high neutron emission rates;

Though OSC(5 ns) and DAQ datasets present the same sampling rate, significantly different results obtained in term of n-γ pulse shape discrimination can be partly explained in terms of different bit resolution. Further measurements with same cabling and amplification will allow for better comparison of the two datasets.

Furthermore since a sensible difference on the rising edge is evident on the OSC(5 ns) average neutron and gamma waveforms, high sampling rate would also allow for the exploitation of the rising edge of the waveforms for n-γ discrimination. This would result in a much faster digital data acquisition system since the waveforms could be recorded up to few samples after the peak.

References

1. Brooks, F. *et al.* Neutron spectrometry — historical review and present status. *Nucl. Instrum. Methods* A**476**, 1–11 (2002).
2. Harvey, J. *et al.* Scintillation detectors for neutron physics research. *Nucl. Instrum. Methods* **162**, 507–529 (1979).
3. Marion, J. *et al.*. (eds.) Fast Neutron Physics, parts 1 and 2 (New York: Interscience) (1960).
4. Birks, J. B. The Theory and Practice of Scintillation Counting (Oxford: Pergamon Press) (1964).
5. Marrone,S. *et al.* Pulse shape analysis of liquid scintillators for neutron studies *Nucl. Instrum Rev. Sci. Instrum. Methods* A **490**, 299–307 (2002).
6. Guerrero,C. *et al.* Analysis of the BC501A neutron detector signals using the true pulse shape *Nucl. Instrum. Methods* A **597**, 212–218 (2008).
7. Ronchi, E. *et al. Nucl. Instr. and Meth.* doi:10.1016/j.nima.2009.08.064.
8. Ronchi, E. *et al. A method for digital processing of pile-up events in organic scintillators.* Nucl. Instrum. Methods A **595**, 512–519 (2008).
9. http://www.testmart.com/sp.cfm/DIGOSC/TEK/TDS3034B.html.
10. Riva, M. *et al.* A novel FPGA-based digital approach to neutron/γ -ray pulse acquisition and discrimination in scintillators, 10th ICALEPCS Int. Conf. on Accelerator & Large Expt. Physics Control Systems. Geneva, 10 - 14 Oct 2005, PO2.041-4 (2005).
11. http://www.python.org/
12. Knoll, G.F. Radiation Detection and Measurement p.680, 3rd Ed., John Wiley & Sons, Inc., (2000).
13. Giacomelli, L. *et al.* Evaluation of a digital data acquisition system and optimization of n-γ discrimination for a compact neutron spectrometer,. 82, 013505 (2011).